Neuropilin-1 modulates vascular endothelial growth factor-induced poly(ADP-ribose)-polymerase leading to reduced cerebrovascular apoptosis

Mey, Lilli ; Hörmann, Mareike ; Schleicher, Nadine ; Reuter, Peter ; Dönges, Simone ; Kinscherf, Ralf ; Gassmann, Max ; Gerriets, Tibo ; Al-Fakhri, Nadia

Abstract: Cerebral ischemia is encompassed by cerebrovascular apoptosis, yet the mechanisms behind apoptosis regulation are not fully understood. We previously demonstrated inhibition of endothelial apoptosis by vascular endothelial growth factor (VEGF) through upregulation of poly(ADP-ribose)-polymerase (PARP) expression. However, PARP overactivation through oxidative stress can lead to necrosis. This study tested the hypothesis that neuropilin-1 (NP-1), an alternative VEGF receptor, regulates the response to cerebral ischemia by modulating PARP expression and, in turn, apoptosis inhibition by VEGF. In endothelial cell culture, NP-1 colocalized with VEGF receptor-2 (VEGFR-2) and acted as its coreceptor. This significantly enhanced VEGF-induced PARP mRNA and protein expression demonstrated by receptor-specific inhibitors and VEGF-A isoforms. NP-1 augmented the inhibitory effect of VEGF/VEGFR-2 interaction on apoptosis induced by adhesion inhibition through the V-integrin inhibitor cRGDfV. NP-1/VEGFR-2 signal transduction involved JNK and Akt. In rat models of permanent and temporary middle cerebral artery occlusion, the ischemic cerebral hemispheres displayed endothelial and neuronal apoptosis next to increased endothelial NP-1 and VEGFR-2 expression compared to non-ischemic cerebral hemispheres, sham-operated or untreated controls. Increased vascular superoxide dismutase-1 and catalase expression as well as decreased glycogen reserves indicated oxidative stress in the ischemic brain. Of note, protein levels of intact PARP remained stable despite pro-apoptotic conditions through increased PARP mRNA production during cerebral ischemia. In conclusion, NP-1 is upregulated in conditions of imminent cerebrovascular apoptosis to reinforce apoptosis inhibition and modulate VEGF-dependent PARP expression and activation. We propose that NP-1 is a key modulator of VEGF maintaining cerebrovascular integrity during ischemia. Modulating the function of NP-1 to target PARP could help to prevent cellular damage in cerebrovascular disease.

DOI: https://doi.org/10.1016/j.nbd.2013.06.009

Neuropilin-1 modulates vascular endothelial growth factor-induced poly(ADP-ribose)-polymerase leading to reduced cerebrovascular apoptosis

Lilli Mey,[a] Mareike Hörmann,[a,b] Nadine Schleicher,[c] Peter Reuter,[c] Simone Dönges,[c] Ralf Kinscherf,[d] Max Gassmann,[e] Tibo Gerriets,[c] Nadia Al-Fakhri [a]

[a] Institute of Laboratory Medicine and Pathobiochemistry, Molecular Diagnostics, Philipps University, D-35043 Marburg, Germany

[b] Clinic for Vascular Surgery, University Clinic of Cologne, D-50924 Cologne, Germany

[c] Heart and Brain Research Group, Dept. of Neurology, Justus Liebig University, D-35385 Giessen, and Kerckhoff Clinic, D-61231 Bad Nauheim, Germany

[d] Institute for Anatomy and Cell Biology, Philipps University, D-35037 Marburg, Germany

[e] Institute of Veterinary Physiology, Vetsuisse Faculty, and Zurich Center for Integrative Human Physiology, University of Zurich, CH-8057 Zurich, Switzerland

Correspondence to: PD Dr. Nadia Al-Fakhri, Institute of Laboratory Medicine, Molecular Diagnostics, Philipps University Marburg, Baldingerstrasse, 35043 Marburg, Germany, phone:+49-6421-5866265, fax:+49-6421-5866189, e-mail:alfakhri@med.uni-marburg.de

Abstract

Cerebral ischemia is encompassed by cerebrovascular apoptosis, yet the mechanisms behind apoptosis regulation are not fully understood. We previously demonstrated inhibition of endothelial apoptosis by vascular endothelial growth factor (VEGF) through upregulation of poly(ADP-ribose)-polymerase (PARP) expression. However, PARP overactivation through oxidative stress can lead to necrosis. This study tested the hypothesis that neuropilin-1 (NP-1), an alternative VEGF receptor, regulates the response to cerebral ischemia by modulating PARP expression and, in turn, apoptosis inhibition by VEGF. In endothelial cell culture, NP-1 colocalized with VEGF receptor-2 (VEGFR-2) and acted as its coreceptor. This significantly enhanced VEGF-induced PARP mRNA and protein expression demonstrated by receptor-specific inhibitors and VEGF-A isoforms. NP-1 augmented the inhibitory effect of VEGF/VEGFR-2 interaction on apoptosis induced by adhesion inhibition through the αV-integrin inhibitor cRGDfV. NP-1/VEGFR-2 signal transduction involved JNK and Akt. In rat models of permanent and temporary middle cerebral artery occlusion, the ischemic cerebral hemispheres displayed endothelial and neuronal apoptosis next to increased endothelial NP-1 and VEGFR-2 expression compared to non-ischemic cerebral hemispheres, sham-operated or untreated controls. Increased vascular superoxide dismutase-1 and catalase expression as well as decreased glycogen reserves indicated oxidative stress in the ischemic brain. Of note, protein levels of intact PARP remained stable despite pro-apoptotic conditions through increased PARP mRNA production during cerebral ischemia. In conclusion, NP-1 is upregulated in conditions of imminent cerebrovascular apoptosis to reinforce apoptosis inhibition and modulate VEGF-dependent PARP expression and activation. We propose that NP-1 is a key modulator of VEGF maintaining cerebrovascular integrity during ischemia. Modulating the function of NP-1 to target PARP could help to prevent cellular damage in cerebrovascular disease.

Keywords

Cerebral ischemia; vascular endothelial growth factor; neuropilin-1; PARP; apoptosis; cerebrovascular disease; rat middle cerebral artery occlusion model.

Abbreviations

A7R, neuropilin-1 inhibitor [ATWLPPR]; Bcl-2, B-cell lymphoma 2 protein; BSA, bovine serum albumin; cRGDfV, αV-integrin inhibitor cyclo-[Arg-Gly-Asp-D-Phe-Val]; EC, endothelial cells; GAPDH, glyceraldehyde-3-phosphate dehydrogenase; $\%HLV_{ec}$, edema-corrected ischemic lesion volume; HUVEC, human umbilical vein endothelial cells; IR, ischemia-reperfusion model; IO, ischemia-occlusion model; ISL assay, in situ-ligation assay; MCAO, middle cerebral artery occlusion; NF-κB, nuclear factor κ-light-chain-enhancer of activated B-cells; NP-1, neuropilin-1; PARP, poly(ADP-ribose)-polymerase; PAS, periodic acid-Schiff reaction staining; SOD-1, superoxide dismutase-1; STATs, signal transducers and activators of transcription; SU5416, tyrosine-kinase inhibitor of vascular endothelial growth factor receptor-2 [3-[(2,4-di-methylpyrrol-5-yl)-methylidene]-indolin-2-one]; VEGF, vascular endothelial growth factor; VEGFR-2, vascular endothelial growth factor receptor-2.

Introduction

Neuropilin-1 (NP-1) is an alternative receptor for vascular endothelial growth factor (VEGF) (Soker et al. 1998). NP-1 functions as a coreceptor to VEGF receptor-2 (VEGFR-2), the main receptor for VEGF on vascular endothelial cells (EC) (Petrova et al. 1999). NP-1 potentiates the effects of VEGF-A(165) binding to VEGFR-2 by increasing the cellular response to VEGF (Soker et al. 1998) and by generating a stronger VEGFR-2 signal (Ballmer-Hofer et al. 2011). Among the VEGF family members, VEGF-A is the strongest apoptosis-inhibiting factor of EC with several splice variants (121, 145, 165, 189, and 206 amino acids) that show different receptor affinities. VEGF-A(165) promotes EC survival, proliferation and migration, but also vascular permeability (Zachary 2001). The cerebrovascular endothelium is prominently involved in many processes with high impact on cerebral ischemia and stroke, such as blood-brain barrier integrity, regulation of arterial tone, inflammation, perfusion and thrombosis (Broughton et al. 2009; Dirnagl et al. 1999). Reduced cerebrovascular perfusion leads to an impairment of the blood-brain-barrier that is reversible, when the cerebral blood flow is restored before cellular damage occurs (Dirnagl et al. 1999). Longer lasting interruptions in perfusion lead to apoptosis of the vascular endothelium (Li et al. 1995) encompassing the breakdown of the blood-brain-barrier with consequent cerebral edema, hemispheral swelling and neuronal damage (Dirnagl et al. 1999; Gerriets et al. 2004). Physiological mechanisms inhibiting endothelial apoptosis therefore not only increase endothelial resistance to pro-apoptotic stimuli, but also support vascular and neuronal integrity (Fisher 2008).

A deeper knowledge on vascular apoptosis in cerebral ischemia is warranted to identify new therapeutic targets in stroke management. This implicates

characterization of the features of apoptosis and cell survival in cerebral vascular cells (Broughton et al. 2009). Apoptosis and cell survival are subject to complex regulation by pro- and anti-apoptotic factors. EC survival is governed by growth factors like VEGF and also by adhesion molecules such as integrins (Zachary 2001). Apoptosis in EC and vascular smooth muscle cells is induced through the inhibition of cellular adhesion with subsequent activation of caspase-3, as we have previously demonstrated (Al-Fakhri et al. 2003a). Caspase-3 transduces apoptosis-inducing signals to the nucleus and induces typical apoptotic features such as DNA degradation by endonucleases or inhibition of DNA repair through cleavage of poly(ADP-ribose)-polymerase (PARP). PARP is a nuclear DNA-binding enzyme that supports DNA strand break repair and counteracts pro-apoptotic deoxyribonucleases (Duriez and Shah 1997).

One of the mechanisms, by which endothelial apoptosis is prevented physiologically is a VEGF-dependent induction of PARP expression and activity, as we have previously demonstrated (Hörmann et al. 2011). PARP is also involved in inflammation and oxidative stress (Virag 2005; Aguilar-Quesada et al. 2007) by modulating the activity of several transcription factors as promoter binding cofactor, like p53, nuclear factor κ-light-chain-enhancer of activated B-cells (NF-κB), and signal transducers and activators of transcription (STATs). The role of PARP in cell death and inflammatory responses depends on the cellular activation state. In oxidative stress situations with excessive and irreparable DNA damage, such as acute inflammation, shock, or severe ischemia, overactivation of PARP leads to intracellular ATP depletion resulting in necrosis. In the absence of overactivation, PARP conveys cellular protection (Virag 2005; Aguilar-Quesada et al. 2007).

The mechanisms behind apoptosis inhibition and regeneration of cerebrovascular integrity in cerebral ischemia remain to be identified. We hypothesized that NP-1 modulates VEGF-dependent processes by adapting the cellular response to VEGF/VEGFR-2 mediated signaling and by regulating PARP expression. In this study, we show that NP-1 is an important modulator of VEGF/VEGFR-2-induced apoptosis inhibition in cerebral ischemia and a regulator of PARP expression influencing cell survival. NP-1 could therefore act as a protective vascular receptor during cerebrovascular insults.

Material and methods

Animals and MCAO model

Ischemia was assessed using a permanent and a temporary middle cerebral artery occlusion (MCAO) model, as described previously (Gerriets et al. 2004). Seventeen male Wistar rats (290 to 350 grams; Harlan Winkelmann, Borchen, Germany) were randomly subjected to different treatment groups: (a) ischemia through MCAO for 90 minutes, followed by reperfusion (IR) after 90 minutes (n=8) compared to (b) sham-operation (n=5). These were supplemented by the groups (c) permanent ischemia through MCAO occlusion (IO) (n=3) and (d) untreated control animal (n=1). In IR, 90 minutes occlusion time was chosen, since this time period of ischemia followed by reperfusion has previously been shown to be the time point for the induction of apoptosis in the vascular endothelium (Li et al. 1995). Animals were anesthetized with 5% isoflurane delivered in air at 3.0 l/min for 2 min, followed by 2–3% isoflurane delivered in air at 0.5 l/min. The right external carotid artery was ligated and transsected, a 4-0 silicone–coated nylon suture was inserted through the external

carotid artery stump and advanced into the internal carotid artery beyond the carotid bifurcation until reaching the anterior cerebral artery, so that blood flow to the MCA was blocked. Reperfusion was induced in IR-animals by removing the suture 90 minutes after MCAO. Neurological evaluation was performed at 0, 4 and 24 h (Gerriets et al. 2004) by a clinical score utilizing ten different motor, coordinative and sensory functions and additionally by the Rotarod test for motoric function (Nedelman et al. 2007). After 24 hours, animals underwent MRI (Bruker PharmaScan 7.0T, 16 cm) under isoflurane anesthesia to determine ischemic lesion size. T2-relaxation-time as a marker for brain water content and lesion-related midline shift were measured to quantify vasogenic edema formation. Computer-aided planimetric assessment of the lesion and hemispheric volumes were performed using image analysis software Image J (National Institutes of Health, NIH), regions of interest in qT2 were defined in the ischemic lesions with PharmaScan software 5.1 (Bruker). The edema-corrected ischemic lesion volume (%HLV_{ec}) was calculated from the infarct volume [cm^3] relative to the hemispheric volumes [cm^3] and then scaled to 100% (Gerriets et al. 2004). After MRI, animals were deeply anesthetized and euthanized. The brains were removed, snap-frozen and analyzed.

Ethics

All procedures were in accordance with the uniform requirements for manuscripts submitted to biomedical journals (http://www.icmje.org). Animal experimentation was approved by the responsible legislative authority and complied with EU animal protection legislation (EU Directive 2010/63/EU for animal experiments, http://ec.europa.eu/environment/chemicals/lab_animals/legislation_en.htm).

Cell cultures

Human umbilical vein EC (HUVEC) (PromoCell), the macrovascular EC line EA.hy.926 and brain microvascular line hCMEC/D3 were cultivated for 2 days (d) to 60-70% confluence with endothelial growth medium without VEGF supplement (Promocell), thereafter incubated as follows:

Incubation protocols

HUVEC, EA.hy.926 and hCMEC/D3 (for flow cytometry) were incubated with recombinant human homo-dimeric VEGF-A(165) or VEGF-A(121) 1-100ng/ml ($5x10^{-11}$ - $5x10^{-9}$M) (Peprotech) over 16 hours (h) to 24h for mRNA isolation, over 20h for apoptosis detection, or over 24h to 6d (with repeated incubations at intervals of 48h) for protein isolation, respectively. These incubation periods were determined in preceding experiments (Hörmann et al. 2011)

After stimulation with VEGF that increases the apoptotic threshold (Hörmann et al. 2011), apoptosis was induced by incubation with αV-integrin inhibitor cRGDfV (cyclo-[Arg-Gly-Asp-D-Phe-Val]) 5µg/ml (Bachem) for 24h inhibiting adhesion to vitronectin (2µg/ml)-coated multiwell plates, blocked with 3% BSA (Al-Fakhri et al. 2003a).

To analyze the function of NP-1 and VEGFR-2, the above mentioned cells were incubated with VEGF-A(165) 10ng/ml in the presence or absence of the peptide inhibitor of NP-1 A7R [ATWLPPR] (Bachem) 10µM and/or the selective VEGFR-2 tyrosine-kinase inhibitor SU5416 [3-[(2,4-dimethylpyrrol-5-yl)-methylidene]-indolin-2-one] (Calbiochem) 10µM in the presence or absence of cRGDfV 5µg/ml.

VEGF signal transduction was studied by VEGF-A(165) 100pg/ml-100ng/ml incubation over short time intervals (15-30-60-120min). Involvement of Akt and JNK was analyzed by incubation with Akt inhibitors triciribine 10µM, isozyme-selective

Akti-1/2 1µM or SAPK/JNK inhibitor SP600125 10µM (Calbiochem), respectively, and VEGF-A(165) 1ng/ml-100ng/ml.

Transcriptional or translational regulation was analyzed by incubating EC with VEGF-A(165) 10ng/ml and actinomycin D (AD) 1µg/ml or cycloheximide (CHX) 2µg/ml (Sigma-Aldrich). Additionally, coincubations were carried out using different combinations of AD or CHX with VEGF receptor and kinase inhibitors.

Controls were conducted in parallel to all experiments using only EC medium (negative control), VEGF-A(165) 10-100ng/ml (VEGF control), cRGDfV (apoptosis control), or VEGF receptor and signaling inhibitors, respectively.

Apoptosis detection

Apoptosis was quantified in cultivated cells by annexin V-FITC/propidium iodide (Immunotech) flow cytometry of 20000 cells/measurement (FACSort, BD Biosciences), as previously described (Hörmann et al. 2011). Apoptotic cells were considered annexin V-positive/propidium iodide-negative signals within pre-defined gating criteria.

In rat brain, apoptosis was detected by in situ-ligation assay (ISL) as described previously (Schoppet et al. 2004). It demonstrates the apoptosis-specific form of DNA fragmentation, i.e. 3' single-base overhang, double-stranded DNA breaks. Briefly, a specific DNA probe was prepared by PCR and purified. Brain transverse cryostate sections (6µm) were acetone-fixed, treated with proteinase K 20 µg/mL, then incubated with the digoxigenin (DIG)-labelled DNA fragment and DNA T4 ligase (Sigma) in a humidified chamber for 1 h at room temperature. For negative control, the DIG-labelled DNA fragment was omitted, for positive control, one slide was pretreated with DNAse I. Probe binding was detected by sheep anti-DIG Fab-

antibody conjugated to alkaline phosphatase (Roche, Mannheim, Germany, 1:500). Color development was performed with NBT/BCIP (nitroblue tetrazolium/5-bromo-4-chloro-3-indolyl phosphate) and 1 mM levamisole (Sigma) for 70 min.

Western Blot

Protein was isolated with AllPrep RNA/protein kit (Qiagen) for cells or RIPA buffer (50mM Tris pH 8,0 containing 150mM NaCl, 1% NP-40, 0,5% sodium deoxycholat, 0,1% SDS, protease inhibitor, Complete, Roche) for tissue lysates. Protein concentration was determined with bicinchoninic acid reagent (Thermo-Scientific) followed by electrophoresis and blotting (Hörmann et al. 2011). Primary antibodies employed were rabbit anti human NP-1 (monoclonal, Epitomics, 1:1000) and goat-anti-human PARP (R&D-Systems, 0.4µg/ml). All blots were normalized to β-actin as loading control stained with mouse-anti-β-actin (clone AC-15, Sigma, 1:20.000). Signal transduction molecules were detected with rabbit antibodies against B-cell lymphoma 2 protein (Bcl-2), Akt, phospho-Akt (Ser473/Thr308), SAPK/JNK, phospho-SAPK/JNK (Thr183/Tyr185), ERK1/2, phospho-ERK1/2 (Thr202/204), p38 MAPK, and phospho-p38 MAPK (Thr180/Tyr182) (Cell Signaling, 1:500). Western blots were evaluated by automated densitometry using the gel analyzing function of Image J software (NIH), as previously described (Gassmann et al. 2009). In Bcl-2 blots, only one specific band was detected and evaluated. In NP-1 blots, the 130 kDa band representing the membrane-bound receptor was evaluated, other bands at 90 and 75 kDa representing soluble NP-1 without receptor function (Gagnon et al. 2000; Cackowski et al. 2004) found in individual IR and IO animals were excluded from analysis. In PARP blots, the band at 116 kD corresponding to intact PARP was evaluated. In protein isolated from rat brain, the bands at 89 and 24 kD

corresponding to PARP cleavage products that are found in apoptotic specimens (Hörmann et al. 2011; Boulares et al. 1999) were additionally evaluated, since apoptosis was present in the IR and IO model.

Real-time RT-PCR

PARP-1 mRNA was quantified by real-time polymerase chain reaction (PCR) using Rotorgene (Corbett). mRNA from cells or tissue was isolated with AllPrep RNA/protein kit (Qiagen) or TriFast reagent (Peqlab) and the concentration calculated from OD_{260}. After DNAse I (Invitrogen) treatment and inactivation, reverse transcription (RT) was performed with Omniscript RT kit (Qiagen). PARP-1 real-time PCR was conducted as recently described (Hörmann et al. 2011).

PARP-1 copy numbers, calculated from threshold cycle (C_T) values, were determined by means of serially diluted external standards that were synthesized by PCR and subsequent purification (Al-Fakhri et al. 2003b) and by $\Delta\Delta$ C_T method. Results were normalized to glyceraldehyde-3-phosphate dehydrogenase (GAPDH) mRNA for cell culture experiments and to lamin A/C (LMNA primers, Qiagen) for brain tissue. Expression stability in EC cultures of the house keeping gene under pro-apoptotic conditions and VEGF stimulation was determined in previous studies (Hörmann et al. 2011; Al-Fakhri et al. 2003b). In cerebral ischemia and reperfusion, GAPDH is upregulated in neurons (Tanaka et al. 2002). We therefore employed lamin A/C (Jung et al. 2012) as a house keeping gene for brain tissue analyses, since RNA was derived from whole tissue homogenates containing all brain cells.

Immunocyto- and immunohistochemistry

HUVEC grown on vitronectin-coated (2µg/ml) glass cover slips were incubated in the presence or absence of VEGF-A(165) 10ng/ml for 2d. Cells were fixed with 4% formaldehyde/PBS, incubated with Image-iT FX-signal enhancer (Invitrogen), then with mouse-anti-human VEGFR-2 (Santa Cruz, clone Y-23, 1µg/ml) and rabbit-anti-human NP-1 (5µg/ml) antibodies 16h at 4°C, thereafter with Alexa Fluor 488- and Cy3-labeled secondary antibodies 1h and DAPI 2µg/ml 20min, finally covered with ProLong Gold antifade reagent (all Invitrogen). Negative controls were conducted with an irrelevant primary antibody or PBS. Immunofluorescence was analyzed by means of an AxioVision microscope with optical sectioning using ApoTome.2 structured illumination technology (Zeiss).

Transverse cryostat sections (6µm) were acetone-fixed, incubated with 5% normal serum/PBS, then with primary antibodies: goat anti-PARP (R&D-Systems, 1:20), goat anti-VEGF (R&D-Systems, 1:50), mouse anti-VEGFR-2 (Santa Cruz, clone Y-23, 1µg/ml), rabbit anti-NP-1 (Invitrogen, 5µg/ml), rabbit anti-cleaved caspase-3 (R&D-Systems,1:1000), goat anti-catalase (R&D Systems, 0,5µg/ml) or rabbit anti-superoxide dismutase-1 (SOD-1) (Santa Cruz, FL-154, 10µg/ml) as markers of oxidative stress, rabbit anti-von-Willebrand-factor (Dako, 1:200) for 2-16h at 4°C. Subsequently, slides were incubated with biotinylated secondary antibodies, streptavidin-alkaline phosphatase-conjugate, Fast Red, and Mayer's haemalum (all Sigma). Negative controls were conducted with an irrelevant primary antibody or PBS. Immunostaining was semiquantitatively evaluated by two investigators.

Sections of rat brain tissue were investigated for glycogen content by PAS (periodic acid-Schiff reaction) staining (Kong et al. 2002) to demonstrate energy depletion caused by ischemia (Brucklacher et al. 2002). Stained whole-mount sections were scanned, red PAS staining was converted to grey scale and densitometrical analysis was carried out with Image J software (NIH) (Kong et al. 2002).

Statistics

For all analyses, 3 to 7 independent experiments were performed in triplicate (PCR) or duplicate (all other experiments) and results were expressed as mean +/- standard error of the mean (SEM). Significance of differences was tested a) by unpaired, two-tailed Student's t-test and additionally b) by two-way-ANOVA analysis with Bonferroni correction. Both statistical methods showed concordant results in all analyses; $p<0.05$ was considered as significant difference, $p<0.01$ as highly significant difference.

Histological specimens were evaluated semi-quantitatively by light microscopy at 200-fold magnification through two experienced investigators independently: Immunohistochemical data were analyzed by counting the number of positive cells (with a specific staining) and identifying the cell type. The apoptotic index was determined by counting the number of ISL positive (dark-blue) nuclei. Analyses were carried out in four fields of view at 200-fold magnification per hemisphere and calculating the mean percentage +/- SEM, respectively.

Results

NP-1 increases apoptosis inhibition induced by VEGF/VEGFR-2 interaction

Preincubation with VEGF-A(165) 1-100ng/ml resulted in a significant reduction of the apoptotic rate compared to non-VEGF-treated EC. VEGF-A(165) increased endothelial resistance to apoptosis induced by cRGDfV that inhibits integrin binding to the vitronectin matrix in HUVEC (Figure 1A) and EA.hy.926 cells. The strongest increase in apoptosis resistance was demonstrated for pre-incubation with VEGF-A(165) over 6d (at 48h-intervals) compared to 24h, matching our previous results (Hörmann et al. 2011). These results were reproduced in human cerebrovascular hCMEC/D3 cells. Preincubation with VEGF-A(121) reduced EC apoptosis induced by cRGDfV significantly less than VEGF-A(165), yet increased the resistance to apoptosis (Figure 1A). VEGF-A(121) binds predominantly to VEGFR-2, but has neglectable binding affinity for NP-1, whereas VEGF-A(165) binds both receptors (Zachary 2001). The binding affinity of VEGF-A(165) is slightly higher for VEGFR-2 than for NP-1, however, VEGF-A(165) will preferentially bind to VEGFR-2/NP-1 complexes leading to an increased potency of VEGF-A(165) over VEGF-A(121) (Whitaker et al 2001). Incubation with VEGF-A(165) alone had no influence on the apoptotic rate, whereas VEGF-A(121) slightly increased apoptosis compared to the negative control (Figure 1A). Incubations with receptor inhibitors SU5416 10µM and/or A7R 10µM, selective antagonists of VEGFR-2 or NP-1, respectively, revealed that blocking NP-1 had no significant influence on the induction of apoptosis resistance through VEGF-A(165) in the presence of cRGDfV. However, simultaneous inhibition of VEGFR-2 and NP-1 or blocking VEGFR-2 alone, respectively, abolished the apoptosis inhibiting effect of VEGF (Figure 1B). Therefore, NP-1 signaling alone in the presence of VEGFR-2 inhibitor could not prevent apoptosis induction

consistent with a VEGFR-2 coreceptor role for NP-1, as explained in detail in the discussion section. The inhibitor SU5416 is selective for VEGFR-2 (IC50 = 1.04 µM) (Fong et al. 1999). A7R is an inhibitor of NP-1 (IC50 = 630 nM) that was first described to bind to VEGFR-2. However, detailed studies revealed a selective inhibition of NP-1 binding to VEGF by A7R and no inhibition of VEGFR-2 binding (Perret et al. 2004). Negative control, A7R inhibitor control (Figure 1B) or incubations only with VEGF-A(165) (data not shown) displayed minimal apoptotic rates. Incubation with SU5416 alone or A7R together with SU5416 with or without VEGF showed a small, non-significant change in the apoptotic rate compared to the negative control (Figure 1B). Taken together, NP-1 augmented the anti-apoptotic VEGF effect conveyed through VEGF/VEGFR-2 interaction as demonstrated by incubations with VEGF isoforms, but importantly, NP-1 did not exert an independent apoptosis-inhibiting effect rather acted as a VEGFR-2 coreceptor, as shown by inhibitor experiments.

NP-1 augments the induction of PARP expression by VEGF

Incubation with VEGF-A(165) 1-100ng/ml over 6d at 48h-intervals caused a significantly higher increase in intact PARP protein (116kD), maximum 120%, compared to incubation with VEGF-A(121) 1-100ng/ml, maximum 80%, as demonstrated by Western blot densitometry normalized to β-actin in HUVEC (Figure 2A). Real-time RT-PCR revealed a significant, 270% increase in PARP-1 mRNA production normalized to the house keeping gene GAPDH mRNA after incubation with VEGF-A(165) for 16h compared to negative control preceding the increase in PARP protein. VEGF-A(121) induced a 180% increase in PARP mRNA that was smaller than the VEGF-A(165) effect (Figure 2A). Therefore, binding of both

receptors by VEGF-A(165) induced a significantly higher increase in PARP expression than binding of predominantly VEGFR-2 by VEGF-A(121) consistent with NP-1's role as a VEGFR-2 coreceptor.

Incubation with VEGF-A(165) and the VEGFR-2 inhibitor SU5416 showed a significant reduction of PARP protein expression compared to incubation with VEGF-A(165) alone in HUVEC (Figure 2B). Coincubation of VEGF-A(165) with the NP-1 inhibitor A7R (in the absence of VEGFR-2 inhibition) had no significant impact on the increase in PARP protein expression induced by VEGF in comparison to incubation with VEGF-A(165) alone. In contrast, combined incubation of VEGF-A(165) with A7R and SU5416 further reduced PARP protein compared to incubation with VEGF and SU5416 (Figure 2B). Incubations with A7R and/or SU5416 alone (inhibitor controls) had no effect on PARP protein expression (Figure 2B). The increase in PARP-1 mRNA production (normalized to GAPDH mRNA) through incubation with VEGF-A(165) only was significantly reduced by coincubation of VEGF with SU5416, with A7R or with both inhibitors, respectively (Figure 2B). Inhibitor controls showed no influence on PARP mRNA production. Thus, NP-1 was demonstrated to augment VEGF-dependent induction of PARP expression as a coreceptor to VEGFR-2. These results were reproduced in the EC line EA.hy.926.

VEGF has previously been described to induce the intracellular apoptosis inhibitor Bcl-2 thereby reducing endothelial apoptosis (Gerber et al. 1998). In the present study, incubation with VEGF-A(165) 10ng/ml produced a 20% increase in Bcl-2 protein that did not reach statistical significance. This increase was smaller than the significant elevation in PARP expression induced by VEGF-A(165) (Figure 2C). This

finding underlined the relevance of the VEGF effect on PARP expression as compared to Bcl-2 expression in the context of apoptosis inhibition.

VEGF-dependent signal transduction leading to the induction of PARP expression was found to be mediated by phosphorylation of Akt and JNK, as demonstrated by Western blot of phosphorylated kinase correlated to total kinase. MAPK p38 and ERK1/2 did not show phosphorylation following stimulation with VEGF-A(165) (Figure 2D). These results were supported by experiments with Akt inhibitors triciribine and Akti-1/2 as well as SAPK/JNK inhibitor SP600125 incubated with VEGF-A(165). Therefore, VEGF-A(165) signaling via VEGFR-2 and NP-1 is conveyed by Akt and JNK activation.

The level of PARP regulation by VEGF, whether transcriptional or translational, was investigated by AD or CHX, respectively. AD significantly inhibited PARP protein and mRNA upregulation by VEGF, whereas CHX did not significantly alter PARP protein or mRNA regulation by VEGF (Figure A online supplement). Incubation with AD only reduced PARP protein expression, whereas CHX had no significant effect on PARP compared to control. Thus, VEGF exhibited its effect on PARP gene expression via VEGFR-2 and NP-1 on the transcriptional and not on the translational level.

NP-1 expression colocalizes with VEGFR-2 upon VEGF stimulation and is abolished by apoptosis

VEGFR-2 and NP-1 were expressed on the cell membrane and uniformly distributed in the cytoplasm of HUVEC cultivated without VEGF supplement (Figure 3). The receptors showed colocalization at several sites of the cell surface, demonstrated by

immunofluorescence using 3D-scanning technique of an optical sectioning microscopic device. Upon stimulation with VEGF, NP-1 colocalized extensively with VEGFR-2, the receptors clustered on the cell surface and in the perinuclear space, supporting the VEGFR-2 coreceptor function of NP-1 (Figure 3). Interestingly, in EC undergoing apoptosis induced by adhesion inhibition with cRGDfV, immuno-detectable NP-1 was dramatically reduced and VEGFR-2 distribution was changed to a disseminated, less intense staining pattern. Only few perinuclear receptor clusters containing colocalized NP-1 and VEGFR-2, probably rests of endocytosed receptor clusters, could be demonstrated in cells undergoing apoptosis (Figure 3). Results in EA.hy.926 cells were comparable. This indicated an organizational and functional loss of VEGF receptor integrity in cells undergoing apoptosis.

Cerebral ischemia is associated with increased NP-1 and PARP expression and related to endothelial apoptosis

The in-vitro data were corroborated by a permanent (IO) and a temporary (IR) rat cerebral ischemia model that were characterized by neuronal and endothelial apoptosis in the ischemic hemisphere, as identified by ISL assay (Figure 4). Both models showed vasogenic brain edema on the ischemic side, accompanied by tissue destruction that was more prominent in the IO model. The edematous lesions corresponded to the lesions found on MRI. In the IR model that underwent reperfusion after 90 minutes, the number of apoptotic endothelial and neuronal cells was significantly increased in the ischemic hemisphere as compared to either the contralateral hemisphere or sham-operated and untreated controls (Figure 4). Individual apoptotic nuclei were detected in the contralateral hemisphere in the vicinity of the cerebral midline, possibly as a consequence of the space occupying

effect due to vasogenic edema formation. Comparable results were demonstrated for IO, however, IR showed a higher rate of apoptotic cells than IO (Figure 4), possibly due to the more pronounced tissue destruction in the ischemic hemisphere of the IO model as seen on the histological sections. This might have reduced the number of vessels and neurons detectable by ISL assay in the IO model leading to an only seemingly lower apoptotic rate.

Neurological evaluation and scoring performed at 0, 4 and 24 h as well as cerebral MRI after 24 h, evaluating T2-relaxation-time and midline shift, revealed clinical and radiological signs of cerebral ischemia with ensuing vasogenic edema formation and cerebral infarction in IR or IO exposed animals. Mean ischemic lesion volume $\%HLV_{ec}$, determined by planimetric analysis of MRI at time point 24 h (Gerriets et al. 2004), was 31.5% ± 18.7% in the IO group and 37.0% ± 10.1% in the IR group. The midline shift at time point 24 h was 0.068 +/- 0.0168 cm in the IO group vs. 0.102 +/- 0.0336cm in the IR group. There were no statistical differences between the groups ($p>0.05$). However, these values were significantly different from sham- and non-operated control animals: mean ischemic lesion volume: 0.0% ± 0.0% and midline shift: -0.012 +/- 0.0198 cm. Clinical scores (Nedelman et al. 2007) after MCAO of the IO and IR groups were significantly different from sham- and non-operated animals ($p<0.01$).

Brain sections analyzed by immunohistochemistry showed increased expression of NP-1 and VEGFR-2 in the endothelium and of NP-1 in neurons of the ischemic hemisphere in IO and IR models (Figure 5A). In the IR model, NP-1 expression of neurons and the endothelium was higher on the ischemic than on the contralateral

side, however, only the number of NP-1 positive vessels was significantly different (Figure 5A, 5B). In IO and IR, we generally observed a significantly higher vascular NP-1 expression in regions of endothelial apoptosis compared to brains of non-operated and sham-operated animals. VEGFR-2 showed a similar expression pattern as NP-1 in vascular structures in the IO and IR model with an increased VEGFR-2 expression on the ischemic compared to the contralateral side, but no VEGFR-2 expression in neurons (Figure 5A). PARP immunostaining was increased in the IO and IR model in both hemispheres in the endothelium as well as in neurons compared to sham-operated and non-operated animals (Figure 5A). In the IR model, PARP immunostaining was significantly higher in the neurons on the ischemic side than on the contralateral side. In EC, there was no difference between the hemispheres (Figure 5B). However, the PARP antibody detects intact PARP and its degradation products so that an increased PARP immunostaining might also be due to neuronal apoptosis induction in the ischemic region accompanied by an increase in PARP degradation products. VEGF expression of pial and glial cells as well as individual neurons in the ischemic hemisphere and weaker in the contralateral hemisphere was demonstrated. In the ischemic hemisphere, increased immunostaining of activated (cleaved) caspase-3, catalase (Figure 5A) and SOD-1 expression were found. Von Willebrand factor staining demonstrated the integrity of the endothelial lining (Figure 5A).

Whole tissue lysates prepared separately from both hemispheres of every individual animal showed an increased NP-1 protein expression in the IR model compared to the controls as demonstrated by densitometry of Western blots. NP-1 expression was higher in the contralateral hemisphere of the IR model compared to the ischemic

hemisphere (Figure 5C). However, the tissue lysates consisted of whole brain tissue and did not allow for differentiation of cell types. Mean values of intact PARP protein (116 kD) were almost identical on both sides and remained unaltered compared to the control animals ($p>0.05$). However, PARP degradation products 89 and 24 kD were increased, especially in the ischemic hemisphere (Figure 5C). Note that an unchanged expression of intact PARP 116 kD under the pro-apoptotic conditions of ischemia indicates a net increase in PARP expression, since PARP is degraded immediately during apoptosis induction mainly into the cleavage products 89 and 24 kD (Duriez and Shah 1997; Boulares et al. 1999) that were moderately increased here. PARP mRNA production (normalized to lamin A/C mRNA) was significantly increased in the IR model in the ischemic as well as in the contralateral hemisphere compared to sham-operated and control animals (Figure 5D), supporting the results on the protein level indicating a net increase in PARP production.

Oxidative stress caused by cerebral ischemia can lead to cellular energy depletion. Glycogen is an important energy reserve of the brain (Brucklacher et al. 2002). Whole-mount cryostate sections of brain tissue from the IR model, sham-operated and control animals were analyzed for the glycogen content by PAS (periodic acid-Schiff reaction) staining and computer-assisted evaluation of scanned sections (Kong et al. 2002). The mean glycogen content of ischemic hemisphere of IR model animals was significantly reduced compared to control, however, the contralateral hemispheres and sham-operated animals also showed slightly reduced glycogen content compared to control (Figure 6). The whole ischemic hemisphere was evaluated for glycogen content, so the mean value represents the ischemic region as

well as the non-ischemic tissue. The ischemic region showed almost no PAS staining (Figure 6), indicating a loss of glycogen reserves and energy depletion in this region.

In summary, NP-1, VEGFR-2 and PARP are increased in cerebral ischemia in the context of oxidative stress and imminent vascular and neuronal apoptosis.

Discussion

Protective therapeutic strategies for cerebral ischemia warrant the characterization of vascular apoptosis to understand the implications for stroke, however, little is known about cerebrovascular apoptosis (Broughton et al. 2009). Defining the mechanisms that regulate endothelial integrity will help to identify possible vascular targets for poststroke therapy. This study investigated mechanisms underlying cell survival in cerebrovascular ischemia.

The most important survival factor for the vascular endothelium is VEGF that has both, beneficial and negative effects on the blood-brain-barrier: Next to inhibiting apoptosis (Zachary 2001), VEGF promotes endothelial migration and proliferation (Kowanetz and Ferrara 2006; Ferrara 2009), but it also induces endothelial hyperpermeability (Dirnagl et al. 1999) as an early response to hypoxia (Schoch et al. 2002). VEGF functions need to be regulated to adapt to situative responses. A possible candidate molecule could be the non-tyrosinkinase VEGF receptor NP-1 that influences the interaction of VEGF with the tyrosinkinase receptor VEGFR-2 (Soker et al. 1998 and 2002). An independent VEGF receptor function of NP-1 (Wang et al. 2007) is still controversial (Ylä-Herttuala et al. 2007).

We hypothesized that NP-1 represents the fine-regulating element in the VEGF/ VEGF receptor system modulating the VEGF response. In this study, we found evidence for the enhancement of important effects of VEGF by NP-1. Apoptosis inhibition and upregulation of PARP expression induced by VEGF via VEGFR-2 were augmented by the coreceptor NP-1. VEGFR2 / NP-1-dependent PARP expression was transduced by Akt and JNK pathways and transcriptionally regulated. NP-1, VEGFR-2 and PARP expression were found to be increased in rat cerebral ischemia models in relation to apoptosis and oxidative stress.

NP-1 is also a semaphorin receptor in neuronal cell guidance (Fujisawa and Kitsukawa 1998) and is expressed, next to vessels, on neurons, T-cells, dendritic cells (Lepelletier et al. 2007; Gu et al. 2003) and migrating cancer cells (Jia et al. 2010). NP-1 transgene and gene deletion mouse models indicate its essential role in angiogenesis, capillary formation, cardiovascular development (Kitsukawa et al. 1997; Kawasaki et al. 1999) and brain vessel formation (Kitsukawa et al. 1995). The role of NP-1 in disease has predominantly been investigated in tumor angiogenesis (Eccles and Welch 2007), but its function in (cerebro-)vascular pathologies is largely unknown. NP-1 expression has been related to neovascularization and angiogenesis in ischemic lesion remodeling in the rat or mouse model (Zhang et al. 2001; Beck et al. 2002), but no evidence exists on its role in acute cerebrovascular disease.

The coreceptor function of NP-1 was supported by experiments with VEGF isoforms: VEGF-A(121) that binds predominantly to VEGFR-2 reduced apoptosis significantly less than VEGF-A(165) that binds to VEGFR-2 and NP-1 (Soker et al. 1998; Whitaker et al. 2001). In receptor inhibitor experiments, simultaneous inhibition of

VEGFR-2 and NP-1 had a greater inhibitory impact than VEGFR-2 inhibition alone, consistent with the coreceptor function of NP-1. However, NP-1 inhibition only had no significant effect in the presence of VEGF, explained by the molecular mechanisms of VEGFR-2 and NP-1 interaction: Both receptors form a complex with differential signaling potency, the coreceptor NP-1 displays a receptor-clustering rather than an affinity-converting function. VEGF-A(165) is thought to bind to VEGFR-2 and, at the same time, to VEGFR-2/NP-1 complexes. VEGF-A(121) only activates VEGFR-2 (Whitaker et al. 2001; Zachary 2001), its binding to NP-1 is probably not functional (Pan et al. 2007). Blocking NP-1 by an inhibitor like A7R will therefore not necessarily lead to a reduced effect of VEGF-A(165) on EC (Starzec et al. 2006), whereas simultaneous inhibition of VEGFR-2 and NP-1 compared to VEGFR-2 inhibition only may rather demonstrate NP-1 coreceptor function (Whitaker et al. 2001). Additionally, NP-1 also interacts with VEGFR-2 via its cytoplasmic domain involving synectin (Prahst et al. 2008) so that extracellular binding of an inhibitor to NP-1 might not entirely block VEGFR-2/NP-1 interaction. Hence, the modulating effects of NP-1 on PARP regulation are better identified by VEGF isoform experiments.

Colocalization of NP-1 and VEGFR-2 demonstrated by immunostaining reflects their functional association on EC (Soker et al. 1998; Giraudo et al. 1998; Petrova et al. 1999). VEGF-induced perinuclear clustering of VEGFR-2 and NP-1 may originate from functional receptor complexes localized to endocytic vesicles containing Rab11 (Ballmer-Hofer et al. 2011). Intracellular NP-1 may also be associated with vesiculo-vacuolar organelles for VEGF-induced transcellular transport (Teesalu et al. 2009). The expression pattern of VEGF receptors demonstrated here changed unexpectedly in cells undergoing programmed cell death with an almost complete disappearance

of immunodetectable NP-1 pointing to a loss of VEGF responsiveness of EC. NP-1 may undergo receptor shedding by ADAM-10 releasing soluble NP-1 from EC into the circulation, whereas ADAM-17 is the sheddase of VEGFR-2 (Swendeman et al. 2008). Remarkably, soluble NP-1 acts as VEGF-antagonist by binding VEGF-A(165) (Gagnon et al. 2000). Thus, reduction of membrane-bound NP-1 enhances the susceptibility of the cerebrovascular bed to apoptosis in two ways: by reduced enhancement of VEGFR-2 signaling and through the inhibition of VEGF functions through soluble NP-1.

VEGF signaling via VEGFR-2 / NP-1 was demonstrated here to be transduced by JNK and Akt leading to transcriptional regulation of PARP expression. Anti-apoptotic signaling pathways of VEGF described previously include VEGFR-2-dependent activation of phosphatidylinositol 3'-kinase / Akt (Gerber et al. 1998, Thakker et al. 1999; Hörmann et al. 2011) and NP-1-dependent activation of this pathway with subsequent inactivation of p53 (Wang et al. 2007). Moreover, JNK activation was described, however it was thought to promote apoptosis counteracted by ERK 1/2 (Gupta et al. 1999). Next to vasoprotection, VEGF was attributed a neuroprotective function (Kilic et al. 2006; Wang et al. 2005) exerted through Akt activation exceeding the negative early VEGF effects like vascular leakage (Kilic et al. 2006).

VEGF induces resistance to apoptosis through PARP, as we have previously shown (Hörmann et al. 2011). In cerebral ischemia, the extrinsic apoptosis pathway results in caspase-3 activation (Zhou et al. 2004) that leads to PARP cleavage (Virag 2005; Boulares et al. 1999). In this study, apoptosis was induced through the adhesion

inhibitor cRGDfV that activates caspases and the extrinsic pathway (Al-Fakhri et al. 2003 a) as a parallel to pathophysiological reactions in cerebral ischemia.
Bcl-2, an inhibitor of the intrinsic pathway of apoptosis, has previously been identified as a target of VEGF (Gerber et al. 1998; Kim et al. 2006). In our experimental settings, PARP was the more prominent target of VEGF than Bcl-2.

The exact mechanisms by which PARP counteracts apoptosis are still unknown, whether by its DNA-regenerating function or by the regulation of gene expression (Virag, 2005). PARP induces DNA repair counteracting pro-apoptotic stimuli and is a cofactor to transcription factors associated with inflammation like NF-κB and STATs (Aguilar-Quesada et al. 2007). However, PARP is a two-faced molecule that can cause necrosis when excessive cellular stress occurs (Aguilar-Quesada et al., 2007). Whether PARP acts anti-apoptotic, pro-inflammatory or pro-necrotic depends on the cell's actual activation state. PARP activity and function are controlled by mechanisms that are not fully known (Virag 2005; Aguilar-Quesada et al. 2007). Here, we propose the modulation of VEGF-induced PARP expression through NP-1.

In the rat MCAO model, vascular and neuronal NP-1 and vascular VEGFR-2 were upregulated within 24 hours after occlusion or occlusion-reperfusion in peri-infarct regions characterized by neuronal and endothelial apoptosis and detection of cleaved caspase-3. For the first time, this study related imminent neuro-vascular apoptosis to an increased expression of NP-1 and VEGFR-2. Surprisingly, NP-1 and VEGFR-2 were upregulated in the ipsilateral *and* contralateral hemisphere. In tissue lysates, overall hemispheral NP-1 expression was significantly higher on the contralateral side, possibly because of a higher number of intact vessels and neurons

compared to the infarct side. In histochemistry, a slightly higher number of NP-1 expressing neurons (non-significant) and EC (significant) was demonstrated on the ischemic side. In the vicinity of apoptotic vessels, NP-1 and VEGFR-2 expressions were highly increased.

Previous studies demonstrated murine cerebrovascular NP-1 expression (Thomas et al. 2008) and related NP-1 to angiogenesis during post-ischemic brain remodeling in longer-term rat (Zhang et al. 2001) and mouse MCAO models (Beck et al. 2002). Increased endothelial VEGFR-2 expression was found in the mouse MCAO model three days after ischemia (Beck et al. 2002), but not in rat acute or chronic cerebral ischemia (Hai et al. 2003; Plate et al. 1999). However, short-term changes in the VEGF/VEGF receptor system may be more relevant to cerebral ischemia, since it responds acutely to vascular impairment by VEGF upregulation in microglia and macrophages (Plate et al. 1999) and in neurons and pial cells after transient MCAO in rats (Hayashi et al. 1997). After chronic or acute cerebral hypoperfusion, the NP-1-binding isoform VEGF-A(165) or rat VEGF-A(164) shows a higher expression than VEGF-A(121) (Hai et al. 2003; Hayashi et al. 1997). In the present study, VEGF was demonstrated in brain vessels on the ipsi- and contralateral side possibly resulting from a higher local binding to VEGF receptors (Plate et al. 1999). VEGF induces the vascular expression of NP-1 via VEGFR-2 (Oh et al. 2002) and may thus inhibit apoptosis in cerebral ischemia.

Vascular apoptosis is triggered by pro-apoptotic factors and radical oxygen species (Fisher 2008; Olmez and Ozyurt 2012) resulting from oxidative stress during cerebral ischemia. Oxidative stress induces catalase and SOD-1 expression (Slemmer et al. 2008; Facchinetti et al. 1998) demonstrated here in the vessels of the ipsilateral

hemisphere. Exuberant oxidative stress leads to cellular energy depletion of NAD^+ and ATP. During ischemia, glycogen is metabolized anaerobically generating ATP (Brucklacher et al. 2002). The reduced mean glycogen content demonstrated in ischemic brain indicates energy depletion (Brucklacher et al. 2002) which relates to an increased risk for PARP overactivation and cell death (Virag 2005; Aguilar-Quesada et al. 2007) in the ischemic brain.

PARP immunoreactivity was increased in vessels and neurons after ischemia compared to control animals with an identical expression level of intact PARP in both hemispheres from whole tissue lysates. Since PARP is degraded immediately during apoptosis (Virag 2005; Aguilar-Quesada et al. 2007), stable expression of intact PARP (116 kD) in regions of apoptosis during cerebral ischemia indicates a net increase in PARP. The increase in PARP cleavage products (89 and 24 kD: Boulares et al. 1999) and in PARP mRNA found in the IR model, especially in the ischemic hemisphere, supports this concept. PARP expression induced by VEGF (Hörmann et al. 2011) may reflect a protective response to imminent vascular and neuronal apoptosis during ischemia. However, overactivated PARP can switch from DNA repair to the enhancement of inflammation and oxidative stress causing cellular damage (Virag 2005; Aguilar-Quesada et al. 2007). PARP expression and activity therefore need stringent control through the factors regulating its production like the VEGF/VEGF receptor system.

Conclusions

Taken together, cerebrovascular ischemia induces a widespread increase of NP-1 and VEGFR-2 and the reactive upregulation of anti-apoptotic VEGF in the brain paralleled by signs of oxidative stress. VEGF induces intracellular PARP production that counteracts apoptosis. As a result of ischemia, exuberant oxidative stress leads to cellular energy depletion, a cause of PARP overactivation and necrotic cell death (Virag 2005; Aguilar-Quesada et al. 2007). To prevent PARP overactivation, the induction of PARP expression by VEGF must be controlled. NP-1 modulates the VEGF-dependent upregulation of PARP and may control the cellular response to ischemia. NP-1 therefore represents the best candidate for a key modulator ensuring the maintenance of endothelial and neuronal integrity in cerebrovascular diseases.

Understanding the mechanisms of apoptosis inhibition could ultimately lead to particular or supplemental therapies targeting cerebrovascular apoptosis. NP-1 is a potential target for anti-apoptotic therapeutic strategies, modulators of NP-1 function could adapt the situative response of the VEGF/VEGF receptor system to oxidative stress during cerebral ischemia and should be evaluated in future studies. Modulation of NP-1 and PARP function is a promising strategy for post-stroke treatment in the management of cerebral ischemia.

Acknowledgements

This work was supported by grants from the Foundation for Pathobiochemistry [06/10] and Else-Kröner-Fresenius-Stiftung [P88/08 // A106/08], Germany, to N. A. The authors declare no influence of the sponsors on this study and no competing financial interests.

The authors wish to thank Tobias Luh, Andreas Hildenberg and Christa Löwer for their help in technical matters and Mariusz P. Kowalewski (Vetsuisse Faculty, University of Zurich) for his helpful comments on the manuscript.

References

Aguilar-Quesada R, Muñoz-Gámez JA, Martín-Oliva D, Peralta-Leal A, Quiles-Pérez R, Rodríguez-Vargas JM, de Almodóvar MR, Conde C, Ruiz-Extremera A, Oliver FJ. Modulation of transcription by PARP-1: consequences in carcinogenesis and inflammation. Curr Med Chem 2007;14(11):1179-1187

Al-Fakhri N, Chavakis T, Schmidt-Wöll T, Huang B, Cherian SM, Bobryshev YV, Lord RSA, Katz N, Preissner KT. Induction of apoptosis in vascular cells by Plasminogen Activator Inhibitor-1 and High Molecular Weight Kininogen correlates with their anti-adhesive properties. Biol Chem 2003a;384(3):423-435

Al-Fakhri N, Wilhelm J, Hahn M, Heidt M, Hehrlein FW, Endisch AM, Hupp T, Cherian SM, Bobryshev YV, Lord RSA, Katz N. Increased expression of disintegrin-metalloproteinases ADAM-15 and ADAM-9 following upregulation of integrins $\alpha 5\beta 1$ and $\alpha v\beta 3$ in atherosclerosis. J Cell Biochem 2003b;89(4):808-823

Ballmer-Hofer K, Andersson AE, Ratcliffe LE, Berger P. Neuropilin-1 promotes VEGFR-2 trafficking through Rab11 vesicles thereby specifying signal output. Blood 2011;118(3):816-826

Beck H, Acker T, Püschel AW, Fujisawa H, Carmeliet P, Plate KH. Cell type-specific expression of neuropilins in an MCA-occlusion model in mice suggests a potential role in post-ischemic brain remodeling. J Neuropathol Exp Neurol 2002;61(4):339-350

Boulares AH, Yakovlev AG, Ivanova V, Stoica BA, Wang G, Iyer S, Smulson M. Role of poly(ADP-ribose) polymerase (PARP) cleavage in apoptosis. Caspase 3-resistant PARP mutant increases rates of apoptosis in transfected cells. J Biol Chem 1999;274(33):22932-22940

Broughton BR, Reutens DC, Sobey CG. Apoptotic mechanisms after cerebral ischemia. Stroke 2009;40(5):e331-e339

Brucklacher RM, Vannucci RC, Vannucci SJ. Hypoxic preconditioning increases brain glycogen and delays energy depletion from hypoxia-ischemia in the immature rat. Dev Neurosci 2002;24(5):411–417

Cackowski FC, Xu L, Hu B, Cheng SY. Identification of two novel alternatively spliced neuropilin-1 isoforms. Genomics 2004;84:82-94

Dirnagl U, Iadecola C, Moskowitz MA. Pathobiology of ischaemic stroke: an integrated view. Trends Neurosci 1999;22:391-397

Duriez PJ, Shah GM. Cleavage of poly(ADP-ribose) polymerase: a sensitive parameter to study cell death. Biochem Cell Biol 1997;75(4):337-349

Eccles SA, Welch DR. Metastasis: recent discoveries and novel treatment strategies. Lancet 2007;369(9574): 1742-1757

Facchinetti F, Dawson VL, Dawson TM. Free radicals as mediators of neuronal injury. Cell Mol Neurobiol 1998;18(6):667-682

Ferrara N. Vascular endothelial growth factor. Arterioscler Thromb Vasc Biol 2009;29(6):789-791

Fisher M. Injuries to the vascular endothelium: vascular wall and endothelial dysfunction. Rev Neurol Dis 2008;5(Suppl1):S4-11

Fong TA, Shawver LK, Sun L, Tang C, App H, Powell TJ, Kim YH, Schreck R, Wang X, Risau W, Ullrich A, Hirth KP, McMahon G. SU5416 is a potent and selective inhibitor of the vascular endothelial growth factor receptor (Flk-1/KDR) that inhibits tyrosine kinase catalysis, tumor vascularization, and growth of multiple tumor types. Cancer Res 1999;59(1):99-106

Fujisawa H, Kitsukawa T. Receptors for collapsin/semaphorins. Curr Opin Neurobiol 1998;8(5):587-592

Gagnon ML, Bielenberg DR, Gechtman Z, Miao HQ, Takashima S, Soker S, Klagsbrun M. Identification of a natural soluble neuropilin-1 that binds vascular endothelial growth factor: In vivo expression and antitumor activity. Proc Natl Acad Sci U S A 2000;97(6):2573-2578

Gassmann M, Grenacher B, Rohde B, Vogel J. Quantifying Western blots: pitfalls of densitometry. Electrophoresis 2009;30:1845-1855

Gerber HP, Dixit V, Ferrara N. Vascular endothelial growth factor induces expression of antiapoptotic proteins Bcl-2 and A1 in vascular endothelial cells. J Biol Chem 1998;273:13313-13316

Gerriets T, Stolz E, Walberer M, Müller C, Rottger C, Kluge A, Kaps M, Fisher M, Bachmann G. Complications and pitfalls in rat stroke models for middle cerebral artery occlusion: a comparison between the suture and the macrosphere model using magnetic resonance angiography. Stroke 2004;35(10):2372-2377

Giraudo E, Primo L, Audero E, Gerber HP, Koolwijk P, Soker S, Klagsbrun M, Ferrara N, Bussolino F. Tumor necrosis factor-alpha regulates expression of vascular endothelial growth factor receptor-2 and of its co-receptor neuropilin-1 in

human vascular endothelial cells. J Biol Chem 1998;273(34):22128-22135

Gu C, Rodriguez ER, Reimert DV, Shu T, Fritzsch B, Richards LJ, Kolodkin AL, Ginty DD. Neuropilin-1 conveys semaphorin and VEGF signaling during neural and cardiovascular development. Dev Cell 2003;5(1):45-57

Gupta K, Kshirsagar S, Li W, Gui L, Ramakrishnan S, Gupta P, Law PY, Hebbel RP. VEGF prevents apoptosis of human microvascular endothelial cells via opposing effects on MAPK/ERK and SAPK/JNK signaling. Exp Cell Res 1999;247(2):495-504

Hai J, Li ST, Lin Q, Pan QG, Gao F, Ding MX. Vascular endothelial growth factor expression and angiogenesis induced by chronic cerebral hypoperfusion in rat brain. Neurosurgery 2003;53(4):963-970

Hayashi T, Abe K, Suzuki H, Itoyama Y. Rapid induction of vascular endothelial growth factor gene expression after transient middle cerebral artery occlusion in rats. Stroke 1997;28(10):2039-2044

Hörmann M, Mey L, Kharip Z, Hildenberg A, Nemeth K, Heidt M, Renz H, Al-Fakhri N. Vascular endothelial growth factor promotes endothelial survival by induction of poly(ADP-ribose)-polymerase expression in the human vasculature. J Thromb Haemost 2011;9:1391-1403

Jia H, Cheng L, Tickner M, Bagherzadeh A, Selwood D, Zachary I. Neuropilin-1 antagonism in human carcinoma cells inhibits migration and enhances chemosensitivity. Br J Cancer 2010;102(3):541-552

Jung HJ, Coffinier C, Choe Y, Beigneux AP, Davies BSJ, Yang SH, Barnes II RH, Hong J, Sun T, Pleasure SJ, Young SG, Fong LG. Regulation of prelamin A but not lamin C by miR-9, a brain-specific microRNA. Proc Natl Acad Sci USA 2012;109(7):E423-431

Kawasaki T, Kitsukawa T, Bekku T, Matsuda Y, Sanbo M, Yagi T, Fujisawa HA. Requirement for neuropilin-1 in embryonic vessel formation. Development 1999; 126:4895-4902

Kilic E, Kilic Ü, Wang Y, Bassetti CL, Marti HH, Hermann DM. The phosphatidyl-inositol-3 kinase/Akt pathway mediates VEGF's neuroprotective activity and induces blood brain barrier permeability after focal cerebral ischemia. FASEB J 2006;20:E307-E314

Kim WU, Kang SS, Yoo SA, Hong KH, Bae DG, Lee MS, Hong SW, Chae CB, Cho CS. Interaction of vascular endothelial growth factor 165 with neuropilin-1 protects rheumatoid synoviocytes from apoptotic death by regulating Bcl-2 expression and Bax translocation. J Immunol 2006;177(8):5727-5735

Kitsukawa T, Shimono A, Kawakami A, Kondoh H, Fujusawa HA. Overexpression of a membrane protein, neuropilin, in chimeric mice causes anomalies in the cardio-vascular system, nervous system and limbs. Development 1995;121:4309-4318

Kitsukawa T, Shimizu M, Sanbo M, Hirata T, Taniguchi M, Bekku Y, Yagi T, Fujisawa H. Neuropilinsemaphorin III/D-mediated chemorepulsive signals play a crucial role in peripheral nerve projection in mice. Neuron 1997;19:995-1005

Kong J, Shepel PN, Holden CP, Mackiewicz M, Pack AI, Geiger JD. Brain glycogen decreases with increased periods of wakefulness: implications for homeostatic drive to sleep. J Neurosci 2002; 22(13):5581–5587

Kowanetz M, Ferrara N. Vascular endothelial growth factor signaling pathways: therapeutic perspective. Clin Cancer Res 2006;12(17):5018-5022

Lepelletier Y, Smaniotto S, Hadj-Slimane R, Villa-Verde DM, Nogueira AC, Dardenne M, Hermine O, Savino W. Control of human thymocyte migration by neuropilin-1/ semaphorin-3A-mediated interactions. Proc Natl Acad Sci USA 2007;104(13): 5545-5550

Li Y, Chopp M, Jiang N, Zhang ZG, Zaloga C. Induction of DNA fragmentation after 10 to 120 minutes of focal cerebral ischemia in rats. Stroke 1995;26:1252-1258

Nedelmann M, Wilhelm-Schwenkmezger T, Alessandri B, Heimann A, Schneider F, Eicke BM, Dieterich M, Kempski O. Cerebral embolic ischemia in rats: correlation of stroke severity and functional deficit as important outcome parameter. Brain Res. 2007;1130(1):188-96)

Oh H, Takagi H, Otani A, Koyama S, Kemmochi S, Uemura A, Honda Y. Selective induction of neuropilin-1 by vascular endothelial growth factor (VEGF): A mechanism contributing to VEGF-induced angiogenesis. Proc Natl Acad Sci USA 2002;99(1):383-388

Olmez I, Ozyurt H. Reactive oxygen species and ischemic cerebrovascular disease. Neurochem Int 2012;60(2):208-212

Pan Q, Chathery Y, Wu Y, Rathore N, Tong RK, Peale F, Bagri A, Tessier-Lavigne M, Koch AW, Watts RJ. Neuropilin-1 binds to VEGF121 and regulates endothelial cell migration and sprouting. J Biol Chem 2007;282(33):24049-24056

Perret GY, Starzec A, Hauet N, Vergote J, Le Pecheur M, Vassy R, Leger G, Verbeke KA, Bormans G, Nicolas P, Verbruggen AM, Moretti JL. In vitro evaluation and biodistribution of a 99mTc-labeled anti-VEGF peptide targeting neuropilin-1. Nuclear Medicine and Biology 2004;31:575–581

Petrova TV, Makinen T, Alitalo K. Signaling via vascular endothelial growth factor receptors. Exp Cell Res 1999;253(1):117-130

Plate KH, Beck H, Danner S, Allegrini PR, Wiessner C. Cell type specific upregulation of vascular endothelial growth factor in an MCA-occlusion model of cerebral infarct. J Neuropathol Exp Neurol 1999;58(6):654-666

Prahst C, Héroult M, Lanahan AA, Uziel N, Kessler O, Shraga-Heled N, Simons M, Neufeld G, Augustin HG. Neuropilin-1-VEGFR-2 complexing requires the PDZ-binding domain of neuropilin-1. J Biol Chem 2008;283(37):25110-25114

Schoch HJ, Fischer S, Marti HH. Hypoxia-induced vascular endothelial growth factor expression causes vascular leakage in the brain. Brain 2002;125(11):2549-2557

Schoppet M, Al-Fakhri N, Franke FE, Katz N, Barth PJ, Maisch B, Preissner KT, Hofbauer LC. Localization of osteoprotegerin, tumor necrosis factor-related apoptosis-inducing ligand, and receptor activator of nuclear factor-κB ligand in Mönckeberg's sclerosis and atherosclerosis. J Clin Endocrinol Metab 2004;89(8):4104-4112

Slemmer JE, Shacka JJ, Sweeney MI, Weber JT. Antioxidants and free radical scavengers for the treatment of stroke, traumatic brain injury and aging. Curr Med Chem 2008;15(4):404-414

Soker S, Takashima S, Miao HQ, Neufeld G, Klagsbrun M. Neuropilin-1 is expressed by endothelial and tumor cells as an isoform-specific receptor for vascular endothelial growth factor. Cell 1998;92:735-745

Soker S, Miao HQ, Nomi M, Takashima S, Klagsbrun M. VEGF165 mediates formation of complexes containing VEGFR-2 and neuropilin-1 that enhance VEGF165-receptor binding. J Cell Biochem 2002;85(2):357-368

Starzec A, Vassy R, Martin A, Lecouvey M, Di Benedetto M, Crépin M, Perret GY. Antiangiogenic and antitumor activities of peptide inhibiting the vascular endothelial growth factor binding to neuropilin-1. Life Sci 2006;79(25):2370-81

Swendeman S, Mendelson K, Weskamp G, Horiuchi K, Deutsch U, Scherle P, Hooper A, Rafii S, Blobel CP. VEGF-A stimulates ADAM17-dependent shedding of VEGFR2 and crosstalk between VEGFR2 and ERK signaling. Circ Res 2008;103(9):916-918

Tanaka R, Mochizuki H, Suzuki A, Katsube N, Ishitani R, Mizuno Y, Urabe T. Induction of glyceraldehyde-3-phosphate dehydrogenase (GAPDH) expression in rat brain after focal ischemia/reperfusion. J Cereb Blood Flow Metab 2002;22(3):280-288

Teesalu T, Sugahara KN, Kotamraju VR, Ruoslahti E. C-end rule peptides mediate neuropilin-1-dependent cell, vascular, and tissue penetration. Proc Natl Acad Sci USA 2009;106(38):16157-16162

Thakker GD, Hajjar DP, Muller WA, Rosengart TK. The role of phosphatidylinositol3'-kinase in vascular endothelial growth factor signalling. J Biol Chem 1999;274:10002-10007

Thomas N, Tirand L, Chatelut E, Plénat F, Frochot C, Dodeller M, Guillemin F, Barberi-Heyob M. Tissue distribution and pharmacokinetics of an ATWLPPR-conjugated chlorin-type photosensitizer targeting neuropilin-1 in glioma-bearing nude mice. Photochem Photobiol Sci 2008;7(4):433-441

Virag L. Structure and function of poly(ADP-ribose)polymerase-1: role in oxidative stress-related pathologies. Curr Vasc Pharmacol 2005;3(3):209-214

Wang Y, Kilic E, Kilic Ü, Weber B, Bassetti CL, Marti HH, Hermann DM. VEGF overexpression induces post-ischaemic neuroprotection, but facilitates haemodynamic steal phenomena. Brain 2005;128:52-63

Wang L, Dutta SK, Kojima T, Xu X, Khosravi-Far R, Ekkerz SC, Mukhopadhyay D. Neuropilin-1 modulates p53/caspases axis to promote endothelial cell survival. PLoS ONE 2007;2(11):e1161

Whitaker GB, Limberg BJ, Rosenbaum JS. Vascular endothelial growth factor receptor-2 and neuropilin-1 form a receptor complex that is responsible for the differential signaling potency of VEGF(165) and VEGF(121). J Biol Chem 2001;276(27):25520-25531

Ylä-Herttuala S, Rissanen TT, Vajanto I, Hartikainen J. Vascular endothelial growth factors: biology and current status of clinical applications in cardiovascular medicine. J Am Coll Cardiol 2007;49:1015-1026

Zachary I. Signaling mechanisms mediating vascular protective actions of vascular endothelial growth factor. Am J Physiol Cell Physiol 2001;280:C1375-C1386.

Zhang ZG, Tsang W, Zhang L, Powers C, Chopp M. Up-regulation of neuropilin-1 in neovasculature after focal cerebral ischemia in the adult rat. J Cereb Blood Flow Metab 2001;21(5):541-9

Zhou C, Yamaguchi M, Kusaka G, Schonholz C, Nanda A, Zhang JH. Caspase inhibitors prevent endothelial apoptosis and cerebral vasospasm in dog model of experimental subarachnoid hemorrhage. J Cereb Blood Flow Metab 2004;24:419-431

Figure legends

Figure 1. Endothelial resistance to apoptosis is augmented by the vascular endothelial growth factor (VEGF) receptor neuropilin-1 (NP-1). (**A**) Pre-incubation of HUVEC with VEGF-A(165) 10ng/ml (6d, 48h-intervals) significantly reduced apoptosis, demonstrated by annexin V/propidium iodide flow cytometry, induced by the αv-integrin inhibitor cRGDfV 5µg/ml compared to cells not pre-incubated with VEGF. VEGF-A(121) 10ng/ml that binds predominantly to VEGF receptor-2 (VEGFR-2) showed a significantly smaller effect on apoptosis inhibition than VEGF-A(165) that binds both receptors indicative of NP-1's coreceptor role in VEGF-induced apoptosis resistance. Data in (A) and (B) are mean +/- standard error of the mean (SEM) of 4-5 independent experiments. Statistical significance of differences is indicated by the p-value (ANOVA).

(**B**) The impact of NP-1 on apoptosis inhibition is supported by receptor antagonist experiments. Pre-incubation of HUVEC with VEGF-A(165) 10ng/ml over 6d inhibited cRGDfV-induced apoptosis; this was blocked by co-incubation with VEGFR-2 inhibitor SU5416 10µM or the combination of SU5416 with NP-1 inhibitor A7R 10µM. In contrast, A7R had no effect on apoptosis inhibition in cells pre-incubated with VEGF-A(165) compared to incubation with VEGF and cRGDfV explained by the specific mechanisms of VEGFR-2/NP-1 interaction (see results and discussion sections). Incubations with VEGF-A(165) and inhibitors (without cRGDfV) showed no apoptosis induction through A7R and a small, non-significant increase in apoptosis through SU5416 or both inhibitors in the presence of VEGF. Control incubations with inhibitors alone (data not shown) showed no significant induction of apoptosis, incubations with inhibitors and cRGDfV had results similar to cRGDfV alone.

Figure 2. NP-1 increases PARP expression induced by VEGF by acting as a VEGFR-2 coreceptor. (**A**) VEGF-A(165) 10ng/ml induced a significantly stronger increase in PARP protein than VEGF-A(121) 10ng/ml demonstrated by Western blot and automated densitometry. PARP protein was normalized to β-actin as loading control. Additionally, VEGF-A(165) had a greater effect on PARP mRNA production than VEGF-A(121), quantified by real-time RT-PCR and normalized to GAPDH mRNA. These data indicate a coreceptor role for NP-1 augmenting VEGF/VEGFR-2-induced PARP expression. Data in (A) - (C) are mean +/- SEM of 3 independent experiments, p-values (ANOVA) are indicated. Representative blots of experiments are supplemented to the densitometry data.

(B) Incubation with VEGF-A(165) and SU5416 (VEGFR-2 inhibitor) demonstrated a significantly reduced expression of PARP protein compared to incubation with VEGF alone or with A7R (NP-1 inhibitor) and VEGF. Combined incubation of A7R and SU5416 with VEGF-A(165) further reduced PARP protein emphasizing the coreceptor function of NP-1. PARP mRNA production was strongly increased by incubation with VEGF-A(165) and blocked by VEGF receptor inhibitors SU5416 and A7R. Incubation with A7R significantly inhibited the VEGF-dependent increase, SU5416 or both inhibitors led to a further reduction of the VEGF effect, however, the differences between PARP mRNA production levels of inhibitor incubations were not statistically significant.

(C) VEGF-A(165) induced the expression of the anti-apoptotic intracellular protein Bcl-2, the expression level was significantly smaller than that of PARP protein and did not reach statistical significance compared to negative control.

(D) Analysis of signal transduction revealed activation of Akt and JNK, whereas ERK1/2 and MAPK p38 remained unphosphorylated. Short term incubations over

15-120 min were carried out with VEGF-A(165) 10-100ng/ml and analyzed by Western blot automated densitometry of the respective phosphorylated to total kinase proteins. Data in (D) are means of 5 independent experiments.

Figure 3. The colocalized receptors VEGFR-2 and NP-1 change their expression pattern upon VEGF stimulation and during apoptosis induction. In control incubations of HUVEC without VEGF ("contr."), VEGFR-2 and NP-1 were demonstrated on the endothelial cell membrane and in the cytoplasm with a disseminated distribution pattern and only occasional colocalization (white arrows). After incubation with VEGF-A(165) 10ng/ml ("VEGF"), clustering and almost complete colocalization of VEGFR-2 and NP-1 was demonstrated by optically sectioned immunofluorescence staining (ApoTome.2, Zeiss). Clusters of colocalized receptors were detectable in the cytoplasm indicating receptor endocytosis. Apoptosis induction with cRGDfV 5µg/ml ("cRGD") dramatically reduced NP-1 expression leaving no NP-1 on the cell surface and only few clusters of NP-1 with VEGFR-2 in the perinuclear space. The VEGFR-2 expression pattern became diffusely distributed in cells undergoing apoptosis. VEGFR-2 is stained green (Alexa Fluor 488), NP-1 red (Cy-3), nuclei are stained blue (DAPI); 600-fold magnification. The scale bar represents 100 µm. A representative example of 3 independent experiments is shown.

Figure 4. Apoptosis of neurons and endothelial cells is detected in the rat model of cerebral ischemia. In the ischemia-occlusion (IO, n=3) and ischemia-reperfusion model (IR, n=8), apoptosis was detected by ISL assay. The number of apoptotic neurons and endothelial cells was significantly higher on the ischemic side of the IR and the IO model compared to sham-operated (n=5) and untreated controls (n=1).

The panels show the IR model stained by ISL assay presenting examples of analyzed neurons and vessels of the ischemic and contralateral side as well as the staining controls (pos: positive control, DNAse I pretreatment; neg: negative control, no probe). Arrowheads in the upper panels indicate ISL-positive, apoptotic neuronal nuclei, arrows in the lower panels indicate the vascular endothelium (200-fold magnification); the scale bar represents 100 µm. Data are means +/- SEM, p-values (ANOVA) are indicated.

Figure 5. Cerebral ischemia of the rat is characterized by changes in NP-1 and PARP expression. (**A**) Cryotome sections of rat brains were stained by immunohistochemistry (alkaline phosphastase-conjugate, Fast Red). Representative examples from the ischemic (Is) and contralateral (Cl) hemisphere of the IR model and of an untreated, normal animal (No) are shown (200-fold magnification). The inserted panels show a close-up of the positively marked vessels at higher magnification. Increased VEGFR-2 and NP-1 immunoreactivity was detected on the endothelium of the ischemic and contralateral hemisphere in the IR model. NP-1 immunostaining was also increased in neurons in the IR model, especially on the ischemic side, compared to controls. PARP immunoreactivity was increased in the endothelium and neurons in IR animals compared to controls. Activated, cleaved caspase-3 (act. casp.-3) and catalase were increased in the vascular endothelium of the ischemic hemishpere indicating a correlation between endothelial apoptosis, increased PARP and NP-1 expression with oxidative stress. Catalase (and SOD-1, not shown) were also moderately increased in vessels of the contralateral hemisphere. As staining controls, von Willebrand factor (positive control for the

endothelial lining) and the negative staining control (neg. contr.) are shown. The scale bar represents 100 µm.

(B) Semi-quantitative evaluation of NP-1 and PARP immunostaining revealed a highly significant increase in NP-1 and PARP positive endothelial and neuronal cells in the IR model on the ischemic (IR ischemic) and contralateral (IR contralat.) side compared to non-operated (no op.) and sham-operated (sham-op.) animals. An increased number of NP-1 and PARP positive vessels were demonstrated in the vicinity of regions of endothelial apoptosis. Comparison of the ischemic and the contralateral hemisphere in IR animals revealed a higher number of NP-1 positive neurons and vessels on the ischemic side, but only endothelial expression was significantly different between the hemispheres. PARP positive vessels were comparably increased in both hemispheres, but a significantly higher count of PARP positive neurons was found in the ischemic compared to the non-ischemic hemisphere.

(C) In separately prepared whole brain tissue lysates of both hemispheres, an increased NP-1 protein expression in the IR model was found compared to controls. NP-1 expression was higher in the contralateral hemisphere than in the ischemic hemisphere demonstrated by Western blot and automated densitometry. Intact PARP protein (116 kD) expression was comparably high in the IR model as in controls, no statistical difference was found between the ischemic and the contralateral hemisphere. PARP cleavage products 89 and 24 kD were moderately increased in the IR model, especially in the ischemic hemisphere. Representative blots of individual animals are supplemented to the densitometry data, actin detection was carried out in the same blot.

(D) The protein data were supported by mRNA results that showed increased PARP mRNA production in the IR model compared to control demonstrated by real-time RT-PCR and normalized to lamin A/C mRNA (the house keeping gene GAPDH, used in cell culture experiments, is regulated in cerebral ischemia, see methods). Data in (B), (C) and (D) are means +/- SEM, p-values (ANOVA) are indicated. These findings indicate a net increase in the production of PARP under pro-apoptotic conditions, since PARP is degraded during apoptosis induction.

Figure 6. Glycogen is depleted in cerebral ischemia. Whole-mount cryostate sections of rat brain stained with PAS (periodic acid-Schiff reaction) for glycogen were scanned and densitometrically evaluated. Ischemic hemispheres of the IR model showed a significantly reduced glycogen content compared to control, however, PAS staining was also slightly reduced in contralateral hemispheres and sham-operated animals compared to controls (the difference just missed statistical significance in contralateral hemispheres). A representative example of PAS staining for tissue glycogen (red stained tissue) is demonstrated in a coronary section of a brain from an IR-treated animal (10-fold magnification). Red staining indicates intact glycogen storage. The ischemic region in the perfusion area of the A. cerebri media in the right hemisphere shows almost no PAS staining caused by tissue glycogen depletion, as indicated by a dotted line.

Figure
Click here to download high resolution image

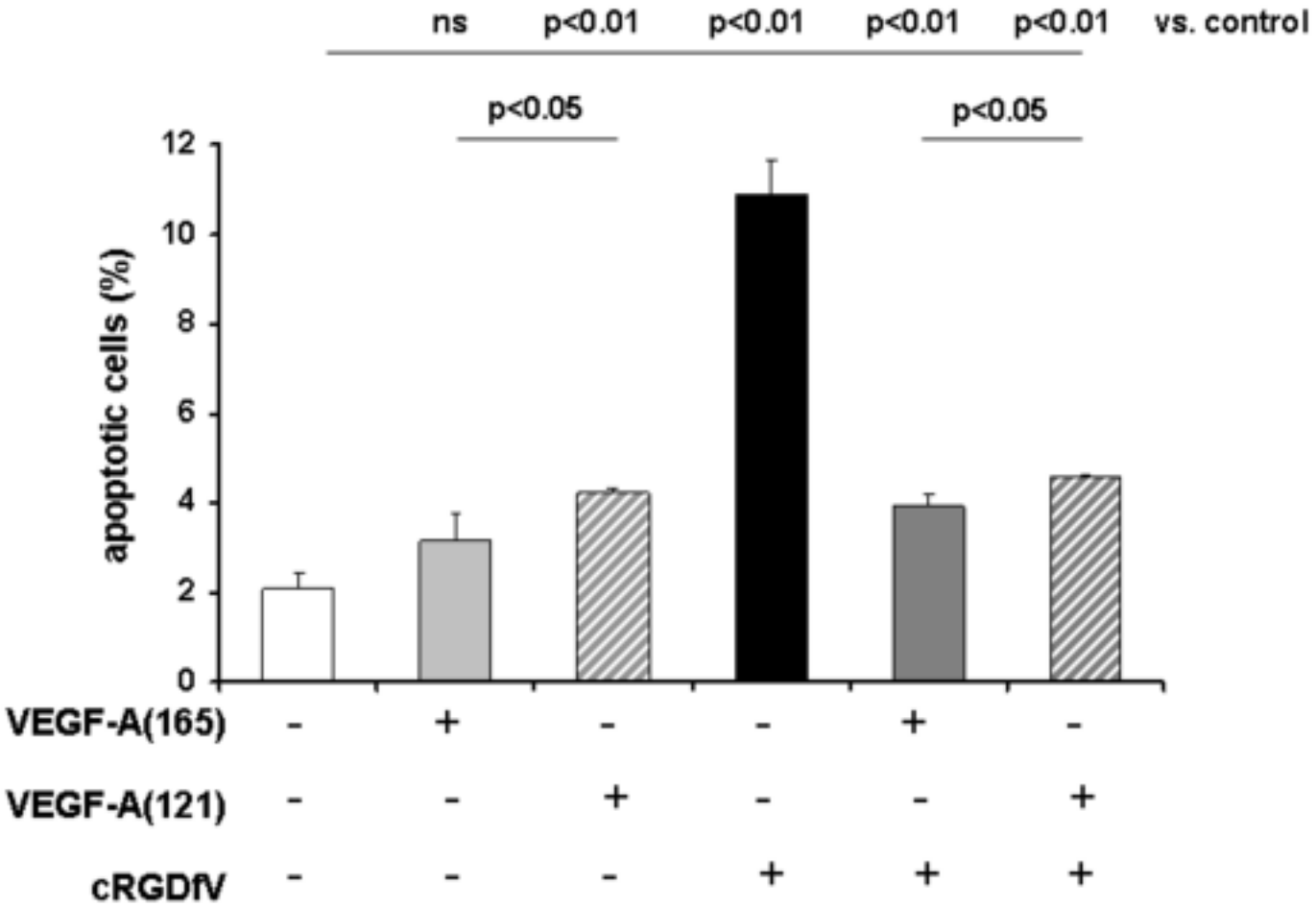

Figure 1A

Figure
Click here to download high resolution image

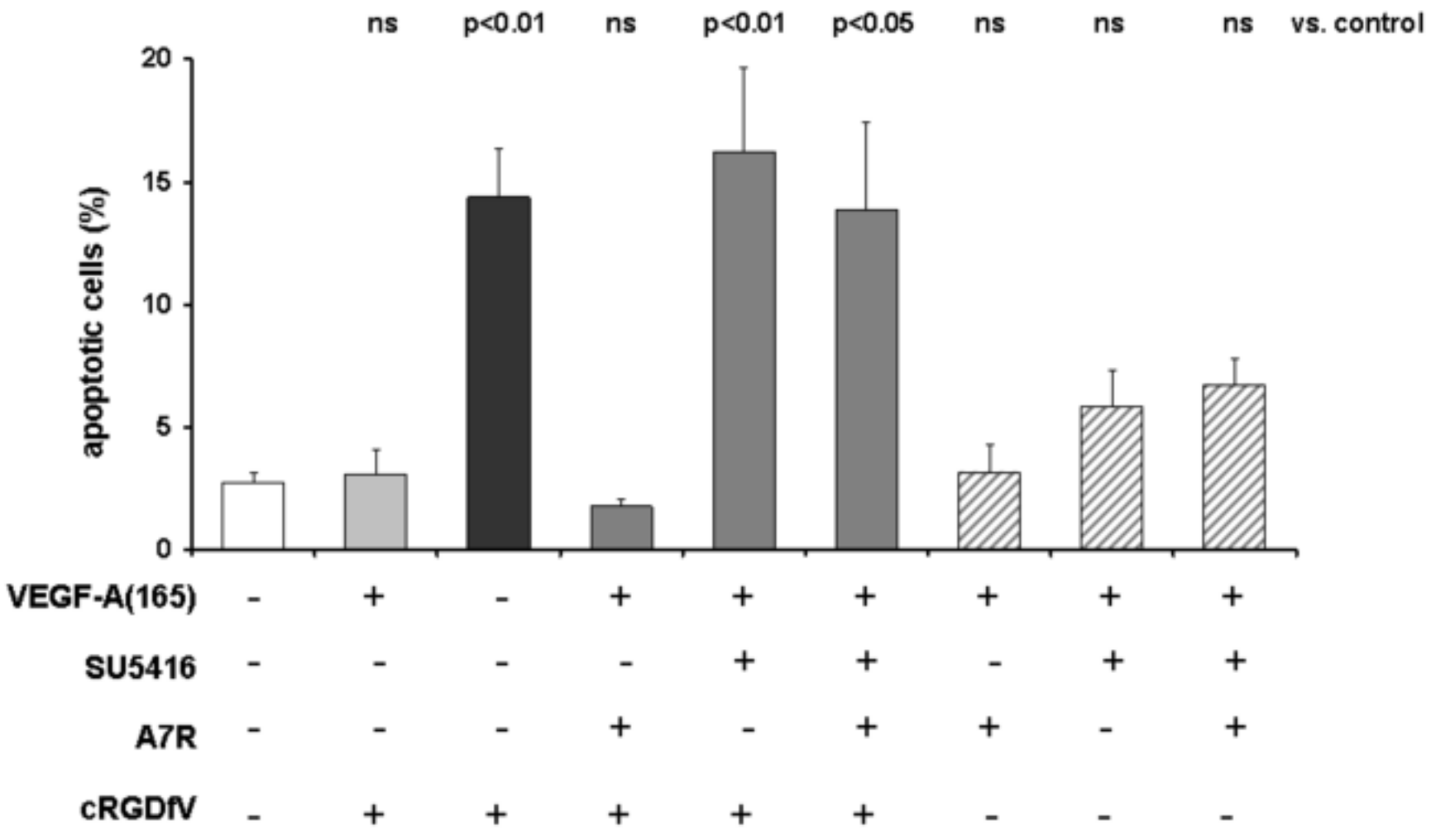

Figure 1B

Figure
Click here to download high resolution image

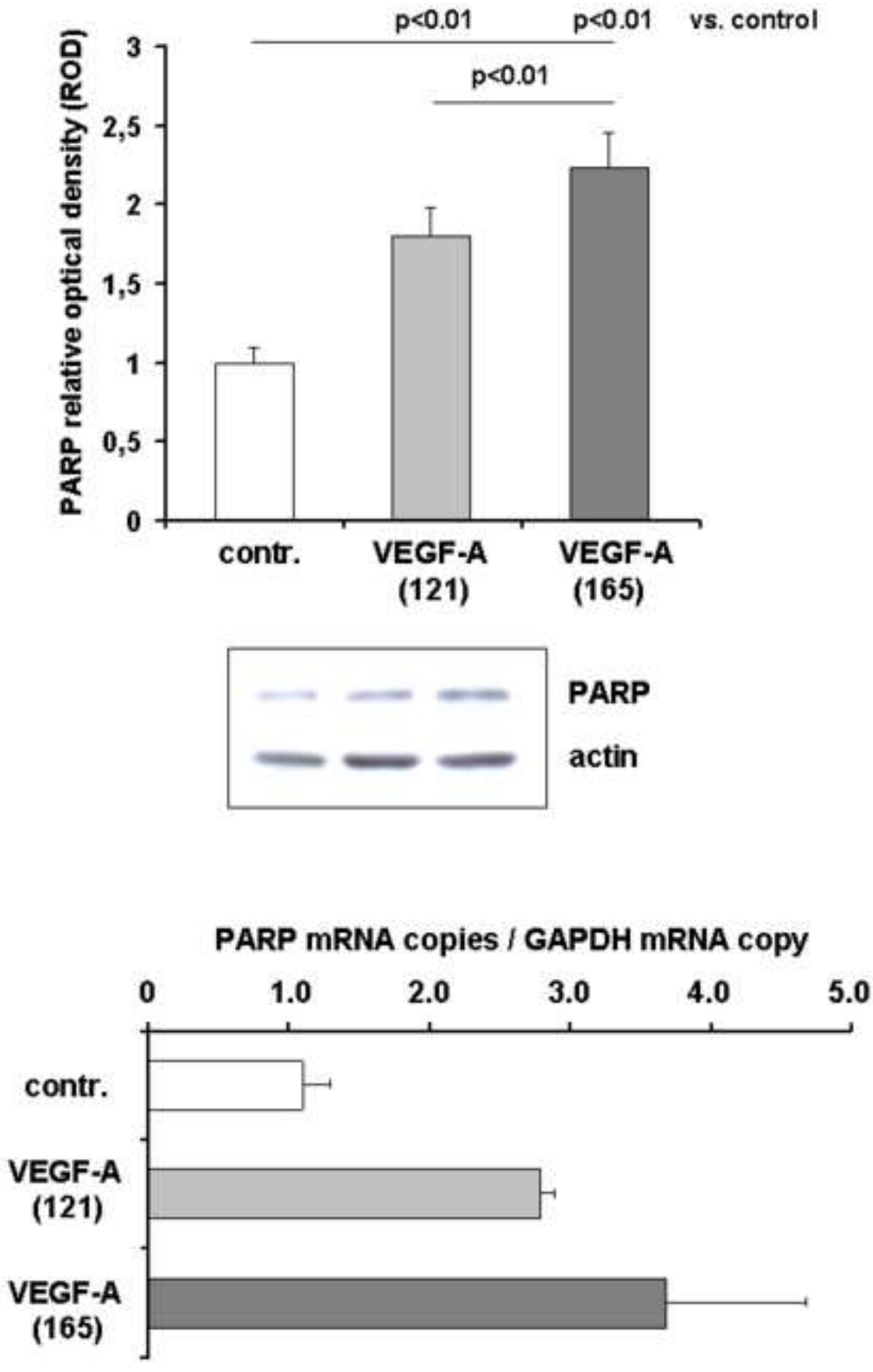

Figure 2A

Figure
Click here to download high resolution image

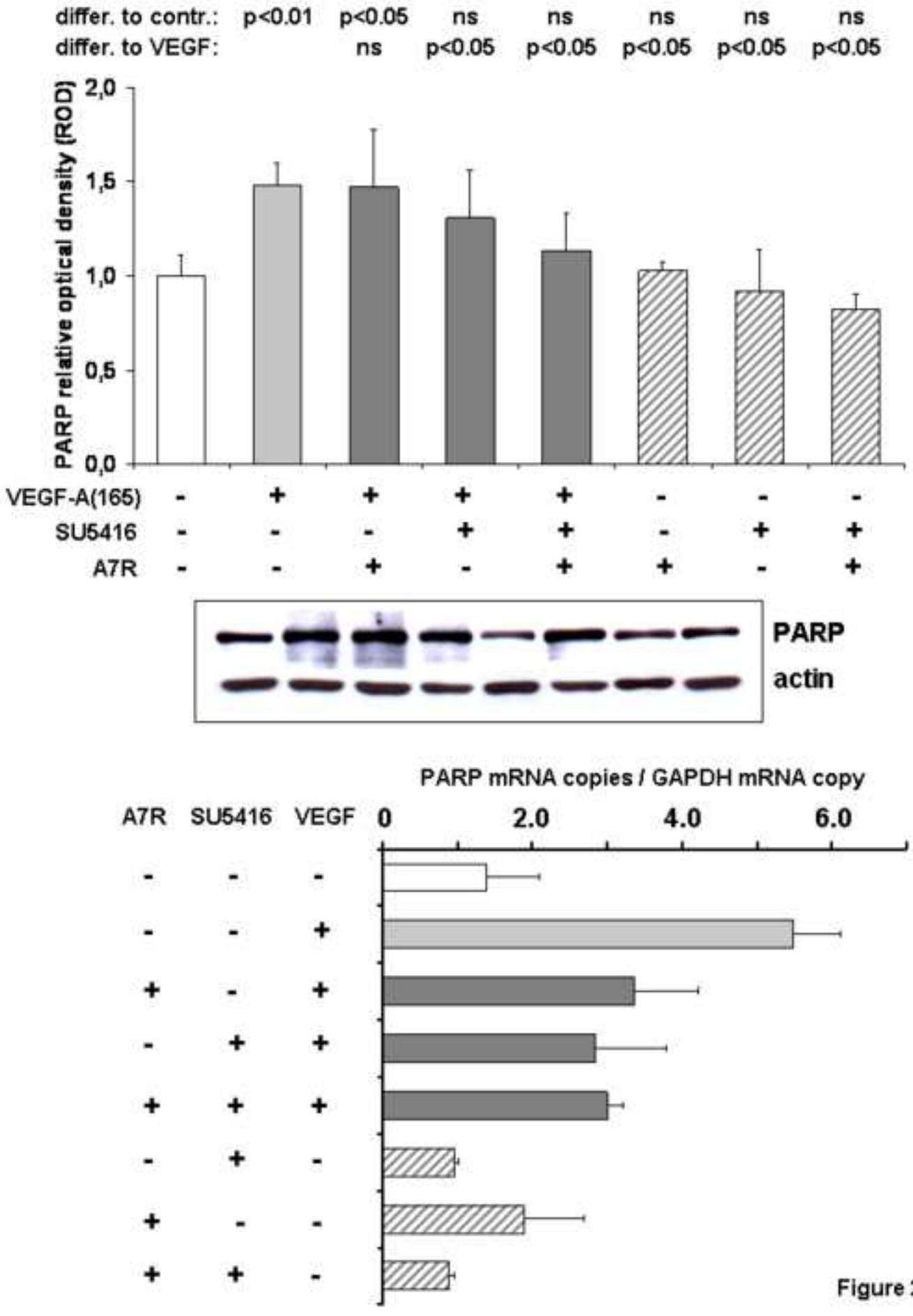

Figure 2B

Figure
Click here to download high resolution image

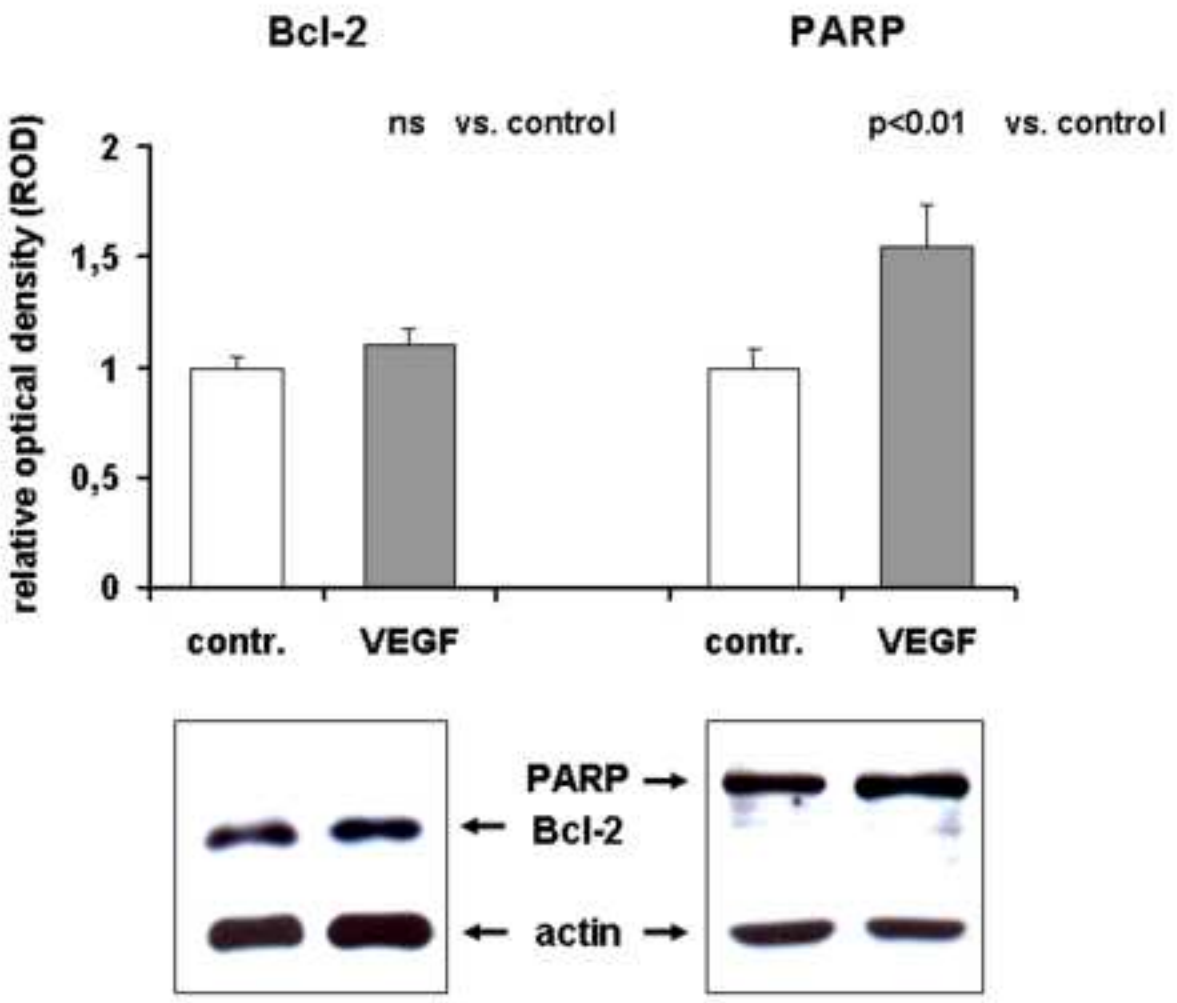

Figure 2C

Figure
Click here to download high resolution image

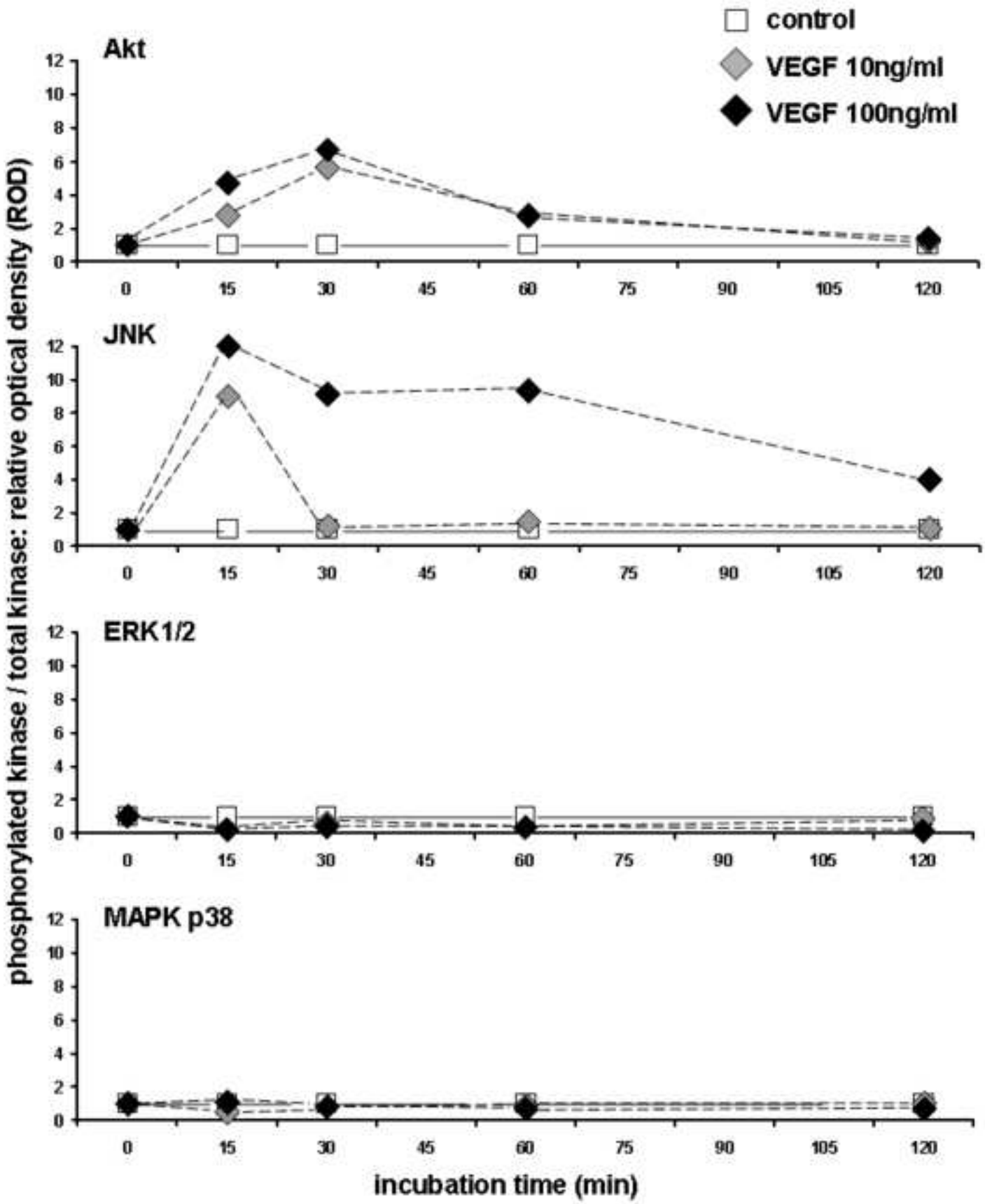

Figure 2D

Figure

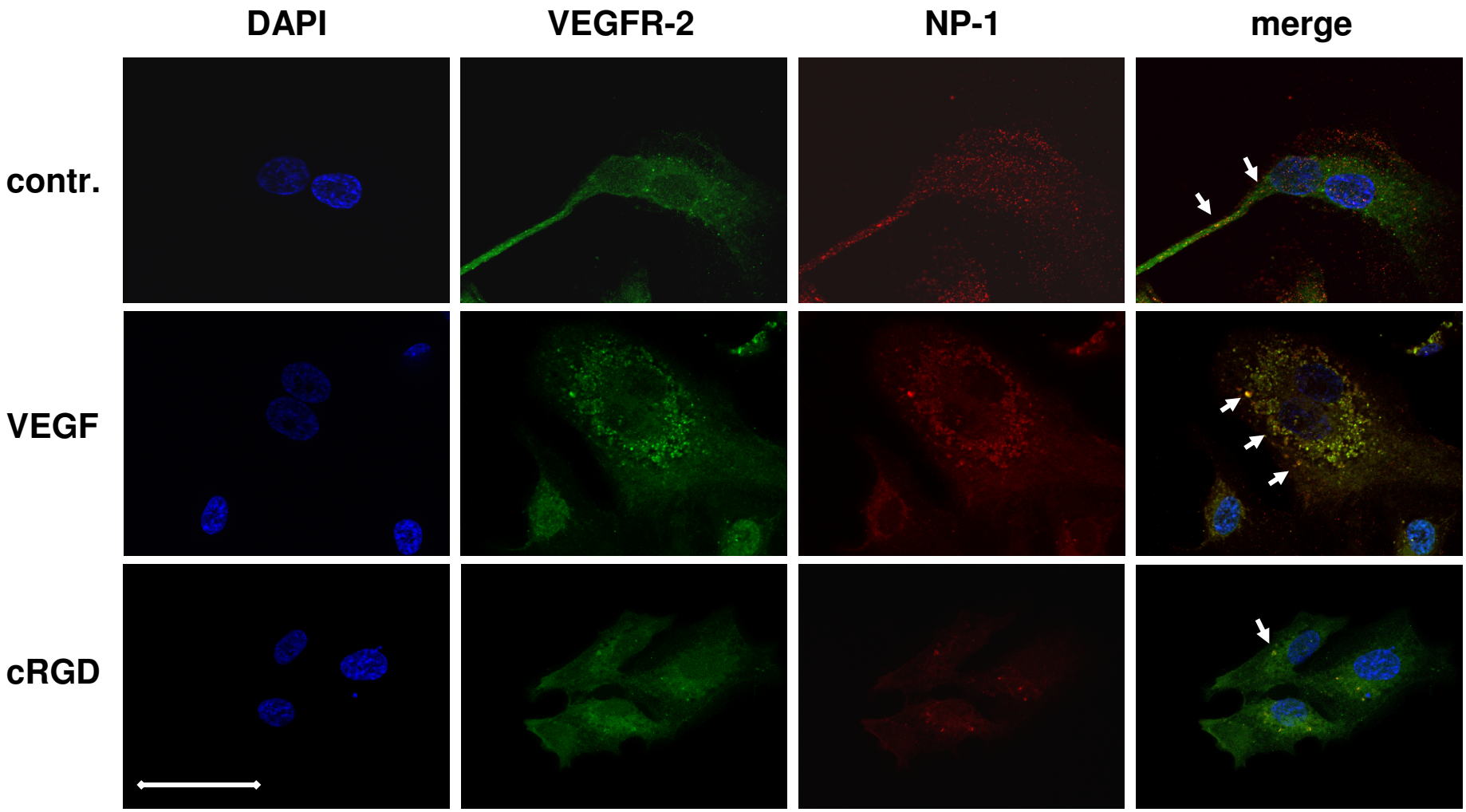

Figure 3

Figure

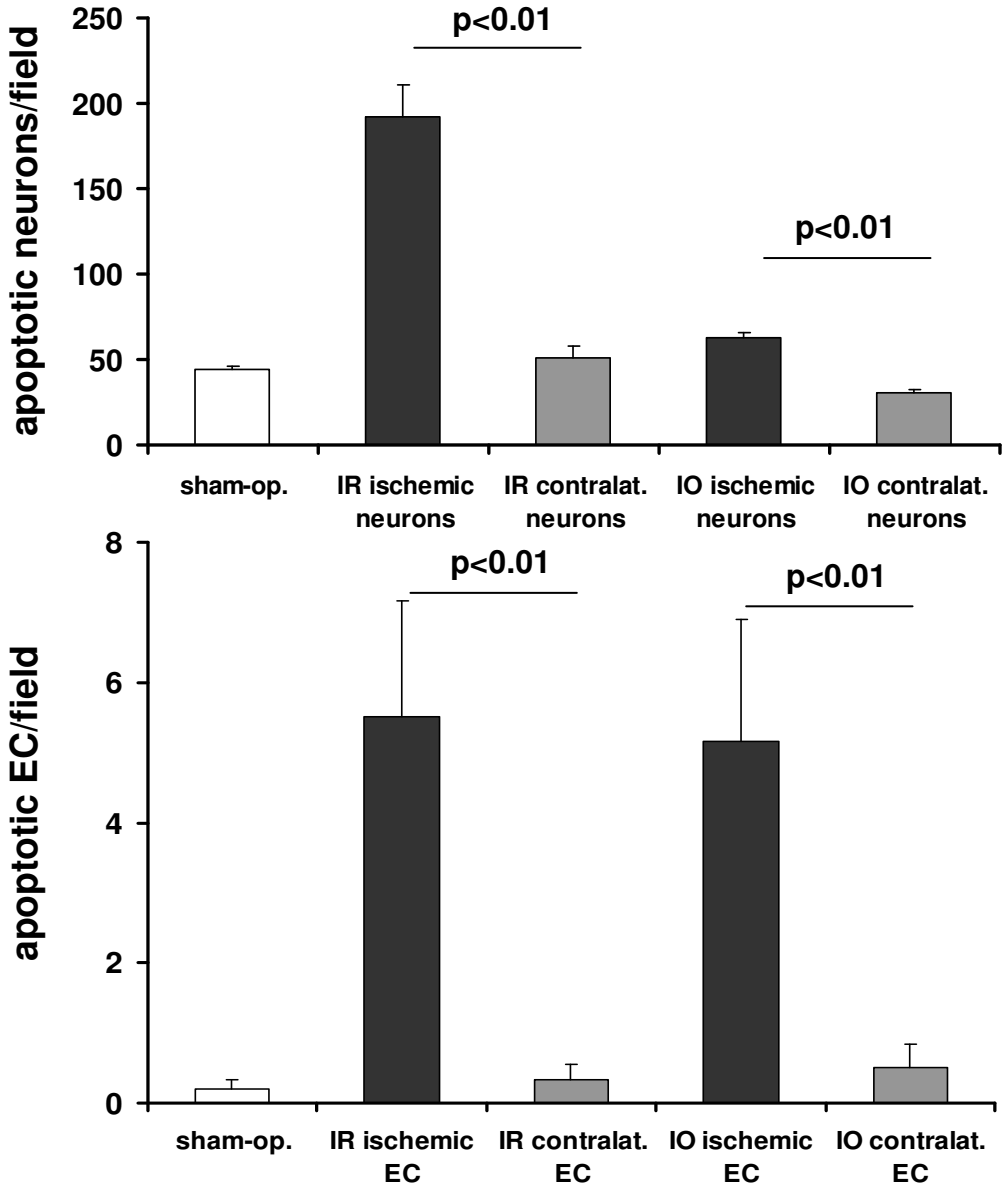

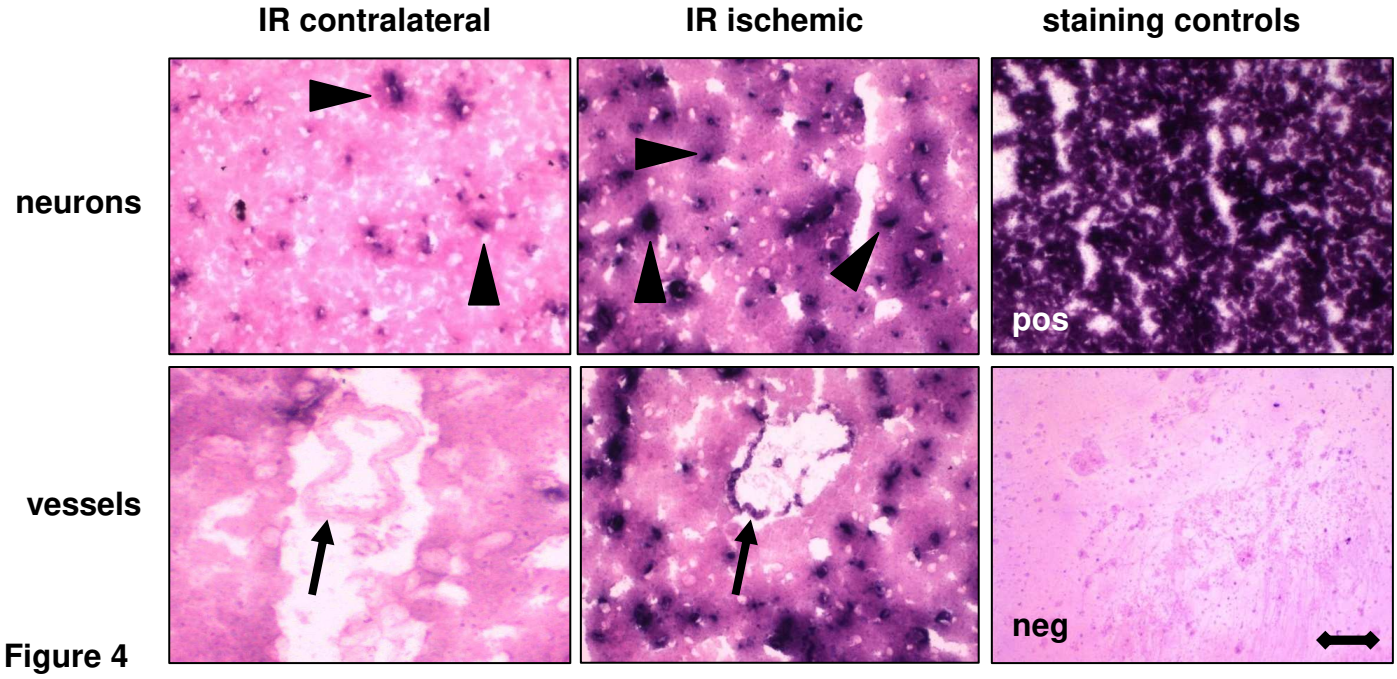

Figure 4

Figure

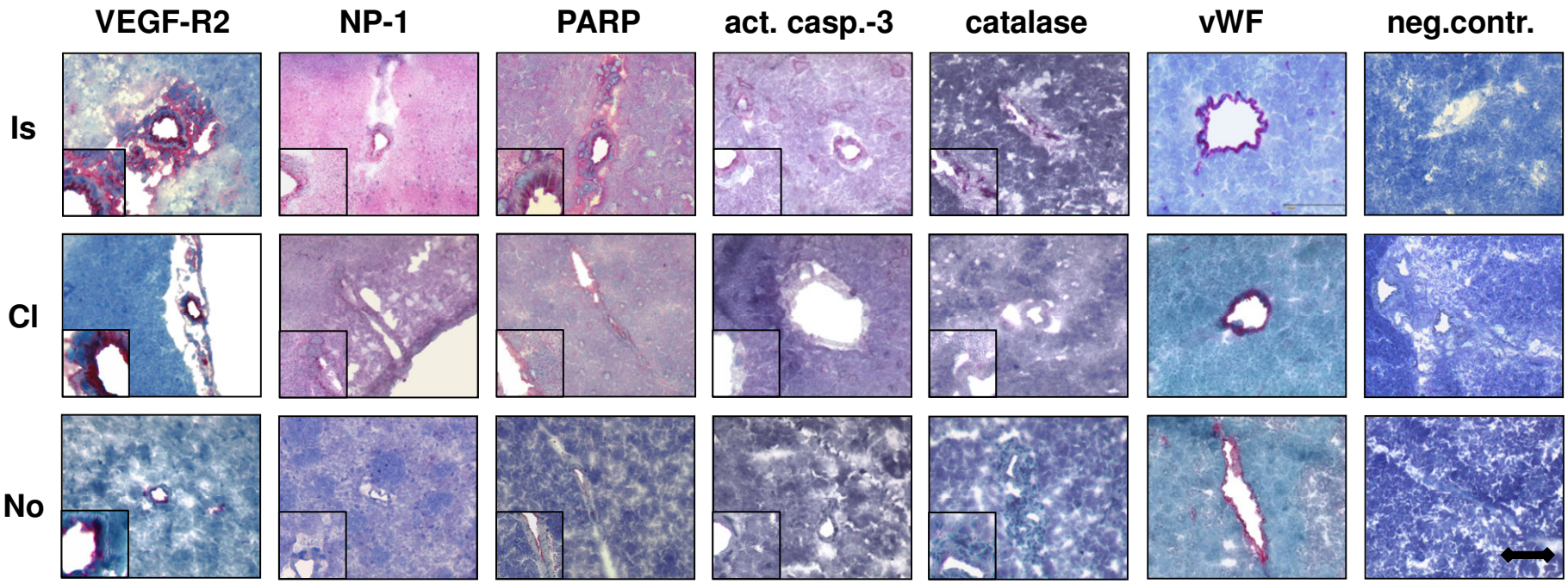

Figure 5A

Figure
Click here to download high resolution image

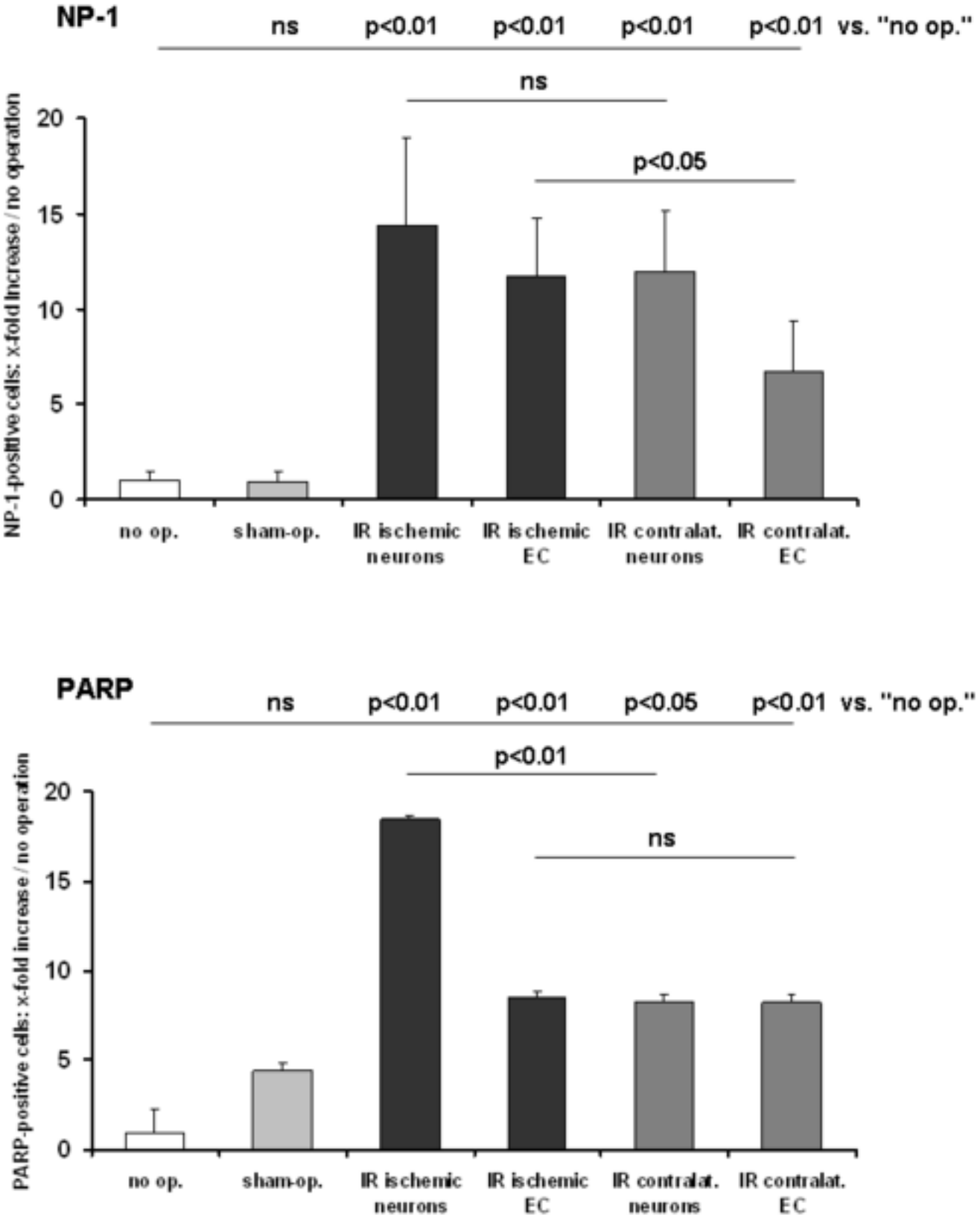

Figure 5B

Figure
Click here to download high resolution image

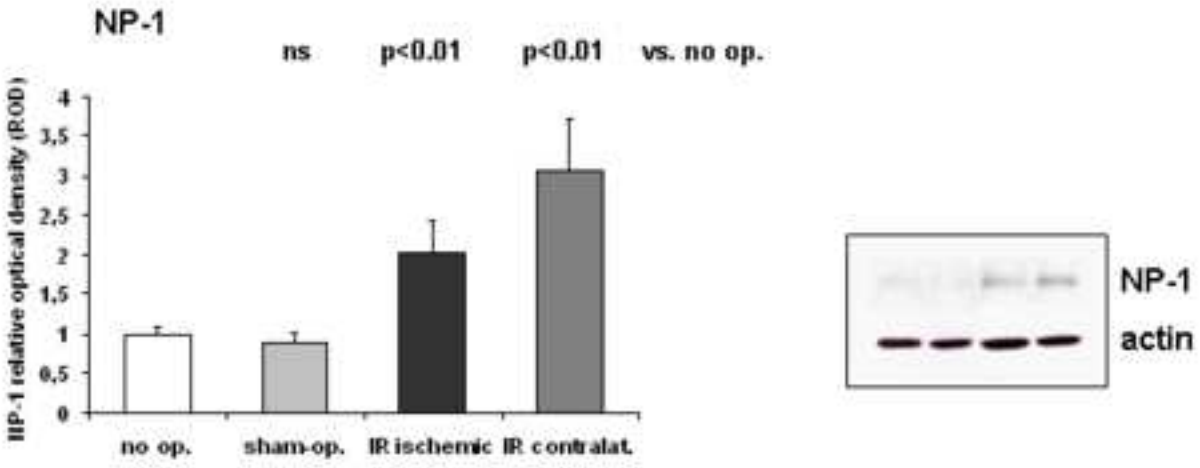

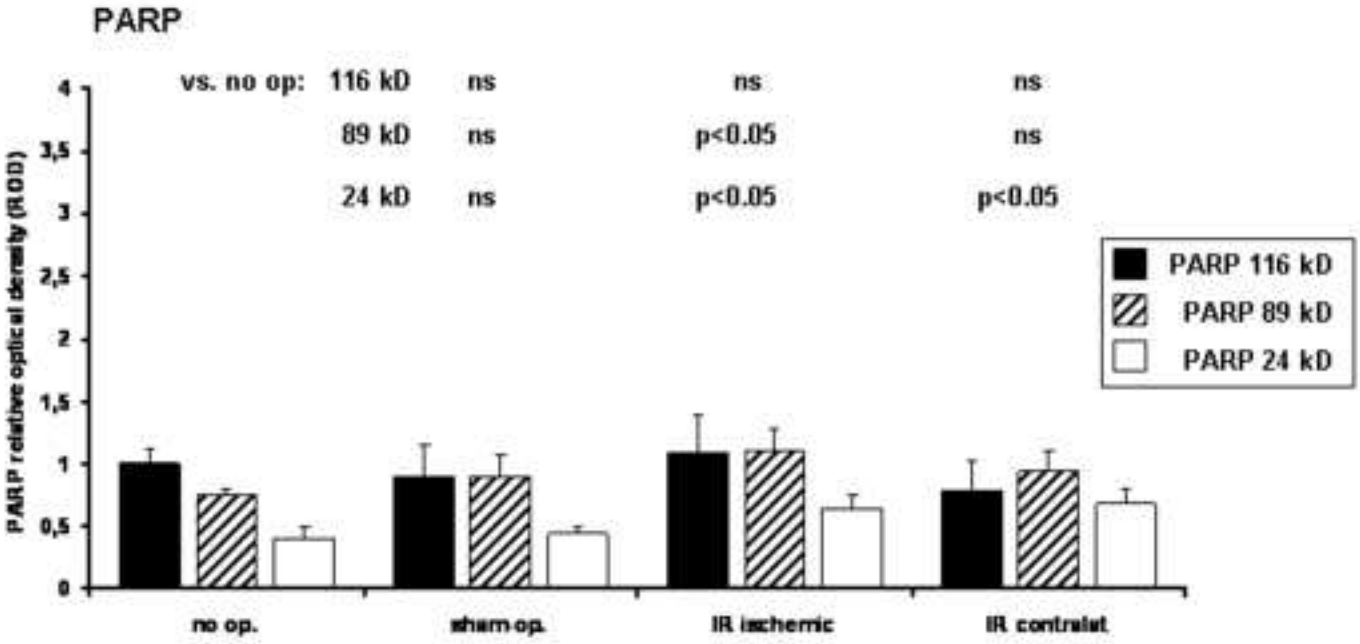

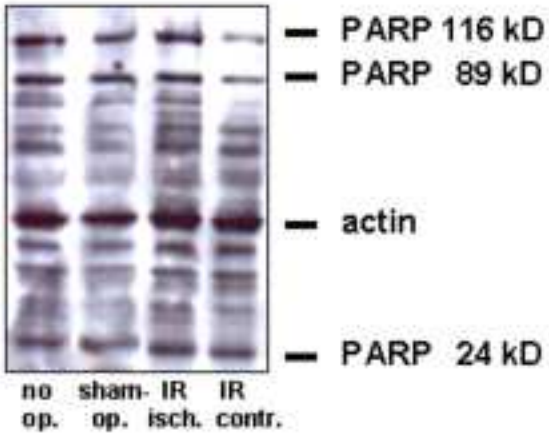

Figure 5C

Figure
Click here to download high resolution image

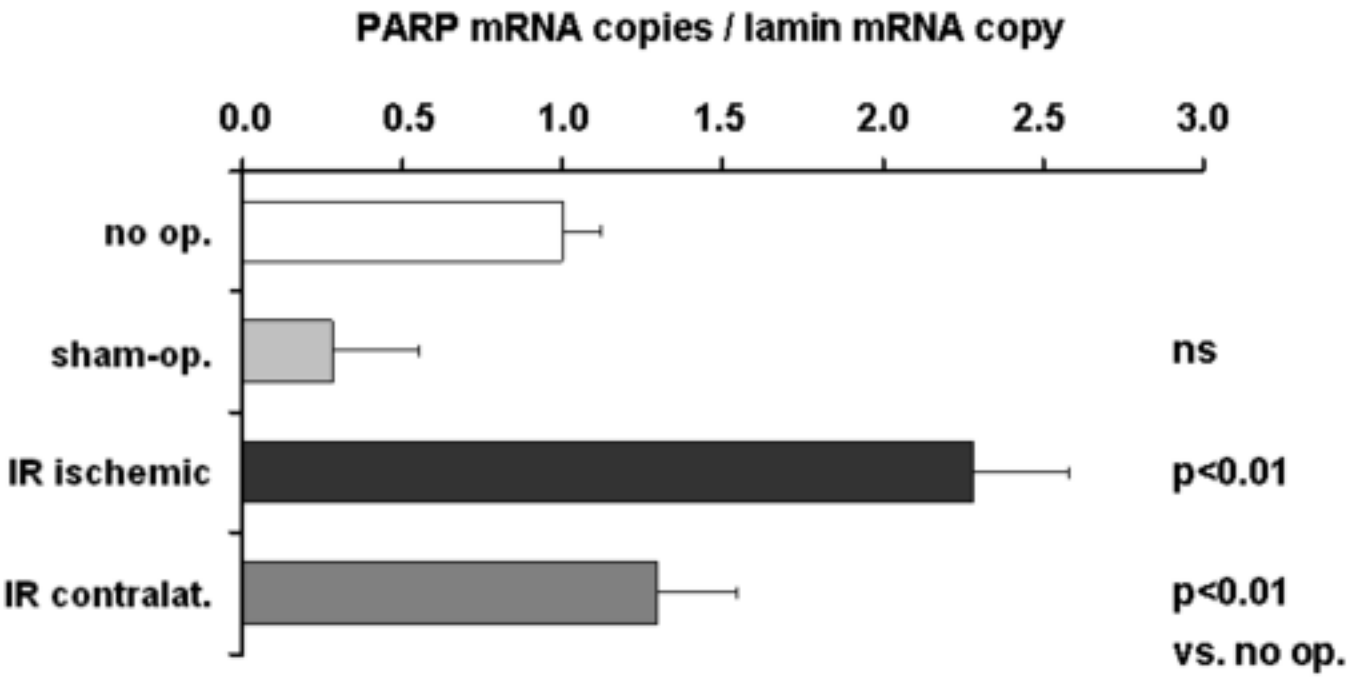

Figure 5D

Figure

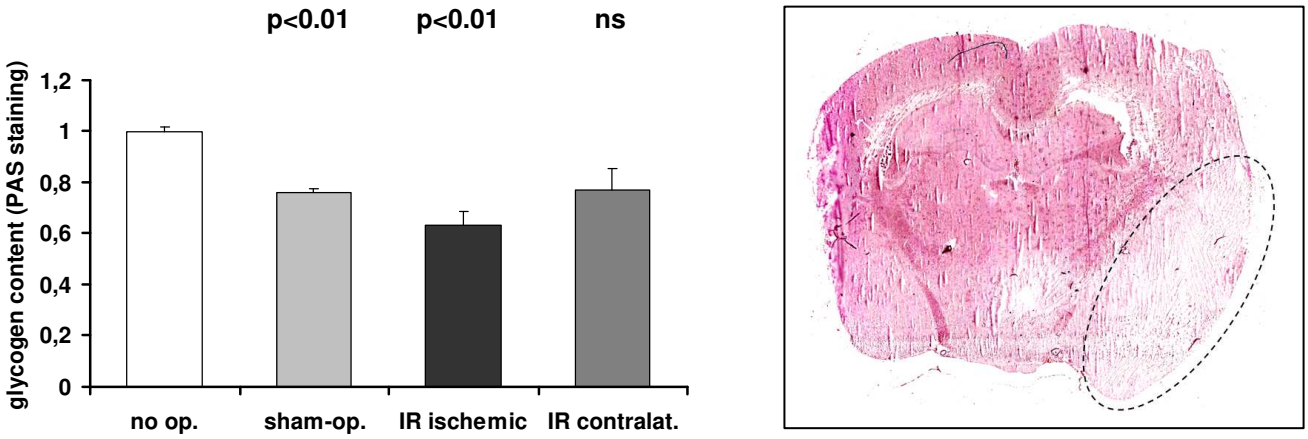

Figure 6

Figure
Click here to download high resolution image

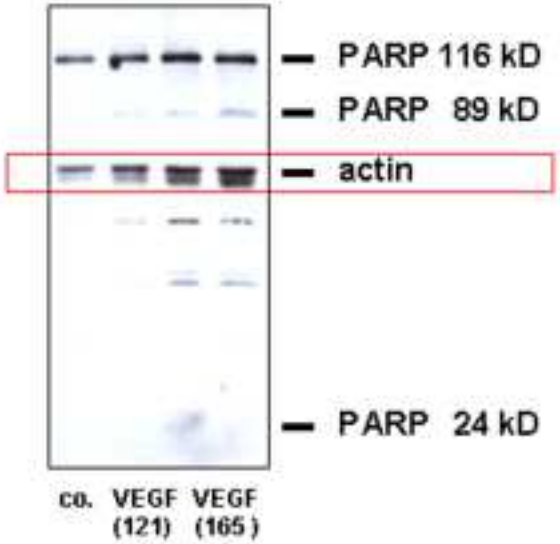

Figure for reviewer. Example of a Western blot of HUVEC incubated with medium only (co.), with VEGF-A(121) or VEGF-A(165) 10 ng/ml, respectively. Intact PARP 116 kD is clearly detectable, whereas the PARP cleavage fragments 89 and 24 kD are not or only faintly detectable. These fragments are caused by apoptosis present at a low rate in endothelial cell culture. Actin was demonstrated in the same blot for the normalization of densitometrical data.

Supplementary Material

Click here to download Supplementary Material: NBD-13-67 online suppl revised.PDF